Journal of Banking and Finance 77 (2017) 78–94

Contents lists available at ScienceDirect

Journal of Banking and Finance

journal homepage: www.elsevier.com/locate/jbf

# Pricing and disentanglement of American puts in the hyper-exponential jump-diffusion model☆

Markus Leippold*, Nikola Vasiljević

*University of Zurich and Swiss Finance Institute, Plattenstrasse 14, 8032 Zurich, Switzerland*

ARTICLE INFO

*Article history:*
Received 12 December 2015
Accepted 14 January 2017
Available online 18 January 2017

*JEL classification:*
G01
G12
G13
C51
C52
C61

*Keywords:*
American options
Early exercise premium
Hyper-exponential jump-diffusion model
Maturity randomization
Jump-diffusion disentanglement

ABSTRACT

We analyze American put options in a hyper-exponential jump-diffusion model. Our contribution is threefold. Firstly, by following a maturity randomization approach, we solve the partial integro-differential equation and obtain a tight lower bound for the American option price. Secondly, our method allows to disentangle the contributions of jumps and diffusion for the early exercise premium. Finally, using American-style options on the S&P 100 index from January 2007 until December 2012, we estimate various hyper-exponential specifications and investigate the implications for option pricing and jump-diffusion disentanglement. We find that jump risk accounts for a large part of the early exercise premium.



## 1. Introduction

The valuation of American options has been one of the most important topics in mathematical finance for almost five decades. A fully analytic solution to the problem, even in the simplest setting, has not yet been obtained whatsoever. The main difficulty stems from the fact that American options allow for an early exercise feature, which requires solving for the option price as a function of a free boundary that is not known a priori. A common approach is to use numerical procedures.[1] However, numerical methods are generally devoid of financial intuition and meaningful interpretations. Moreover, their implementation is often computationally expensive, even more so when we leave the classical Black and Scholes (1973) setting.

A huge part of the literature on analytic pricing of American options in non-Gaussian settings deals with perpetual American options, which can be solved in closed-form under certain assumptions regarding the jumps of the underlying process, and because the early exercise boundary is flat.[2] Moreover, they very often exclude the possibility of overshooting a predefined constant barrier by confining jumps to be always in the opposite direction from the barrier. Hence, many models are based on spectrally one-sided Lévy processes in order to utilize renewal-type integral equations or fluctuation identities. The possibility of an overshoot of the exercise boundary poses several mathematical problems. We need not only an exact distribution of the overshoot, but also the dependency structure between the overshoot and the first passage time. Moreover, for finite-maturity American options, the optimal stopping time is actually a first passage time of an unknown non-uniform space-time boundary.

☆ We thank the Carol Alexander (the editor) and two anonymous reviewers for their constructive comments. We also thank Chris Bardgett, Marc Chesney, Peter Christoffersen, Jakša Cvitanić, Jérôme Detemple, Antonio Mele, András Sali, George Skiadopoulos, and the seminar participants of the Brown Bag Lunch Seminar at the Department of Banking and Finance Institute at the University of Zürich, the Gerzensee Swiss Finance Institute PhD workshop, the Bachelier 2012 Finance Conference, and the University of Zürich and ETH Zürich joint Fin & Math Doc seminar. We gratefully acknowledge financial support from the Swiss Finance Institute (SFI) and Bank Vontobel.

* Corresponding author.
*E-mail addresses:* markus.leippold@bf.uzh.ch (M. Leippold), nikola.vasiljevic@bf.uzh.ch (N. Vasiljević).

[1] Broadie and Detemple (2004) and Detemple (2005) provide a comprehensive overview of different pricing methods for American-style options.

[2] See, e.g., Boyarchenko and Levendorskiĭ, 2002; Mordecki, 2002; Chesney and Jeanblanc, 2004; Alili and Kyprianou, 2005 and references therein.

http://dx.doi.org/10.1016/j.jbankfin.2017.01.014
0378-4266/

Our first goal in this paper is the valuation of finite-maturity American put options in the hyper-exponential jump-diffusion model (HEJD) introduced by Lipton (2002). The logarithm of the asset price is assumed to follow a process, which is a mixture of a drifted Brownian motion and a compound Poisson process with an arbitrary number of positive and negative types of exponentially distributed jumps of finite activity.[3] We choose to work in this particular framework, because it is flexible enough to capture the main empirical features of asset returns and option prices.[4] Furthermore, due to the memorylessness of the exponential distribution, analytic pricing and hedging of vanilla and certain exotic options in a HEJD framework is feasible, hence making this model a plausible candidate for our purpose.

To derive the price of an American put, we adopt a maturity randomization approach. We study the Laplace-Carson transform with respect to the time to maturity of the partial integro-differentialequation (PIDE) and the corresponding initial and boundary conditions describing the dynamics of the American option price. Instead of using a sequence of Erlangian random variables suggested in Carr (1998), we rely on a different sequence of random variables following a distribution suggested in queueing theory literature by Gaver (1966). Both approaches converge pointwise to Dirac's delta function centered at the residual maturity. However, while Carr's maturity randomization requires to solve recursively a set of differential equations, the alternative randomization approach relies on the computation of the Gaver's functionals, resulting in a much simpler and faster computational procedure. For option pricing applications, the alternative randomization approach was studied in, e.g., Kou and Wang (2003); Sepp (2004); Kimura (2010), and Hofer and Mayer (2013). However, American options have not yet been priced using this method. Hence, our results represent a genuine contribution to the existing literature on maturity randomization.[5] We support our theoretical results with numerical examples and demonstrate that our approach represents a fast and accurate pricing engine.

Our second contribution is concerned with analyzing the importance of jump risk for American options. Although we borrow the syntax "disentanglement of diffusion from jumps" from Aït-Sahalia (2004), the semantics is quite different in our study. While Aït-Sahalia (2004) takes an econometric perspective and studies the effect of jumps on the estimation of the diffusion component in asset returns using high-frequency data, we study the implications of a possible overshoot for the early exercise premium. By combining the martingale approach and the PIDE method in the Laplace transform framework, we can disentangle the contribution of jumps and diffusion for the American early exercise premium. Our disentanglement result pertains to the risk-neutral world and is model-dependent in the sense that it relies on the assumption that the underlying process has both diffusion and finite activity jump components. However, unlike econometric approaches, it holds irrespectively of the data frequency.

The impact of jumps on American option prices has been recently considered in Chiarella and Ziogas (2009). They examine jump effects by comparing the shape of the early exercise boundary with and without jumps, keeping the overall volatility constant. In contrast, we consider the disentanglement of jumps and diffusion directly by analytically decomposing the early exercise premium into the respective contributions. Hence, we do not need to rely on a moment-based condition. More importantly, our approach does not require the use of different models, which may distort the inference due to model misspecification. In our setting, we can disentangle jumps from the diffusion component within the same model. Therefore, to the best of our knowledge, our disentanglement idea for American options has not been previously studied in the literature.

Finally, as our third contribution, we estimate a range of HEJD models using American options on the S&P 100 index to provide more intuition and to demonstrate the disentanglement of jumps from diffusion on real data. We focus on short-term options with time to maturity of up to two months and perform sequential (weekly) calibration via penalized weighted nonlinear least squares. The chosen data set and the sequential calibration allow us to study the time variation in the model parameters. Since our sample includes the recent financial crisis, we can study the importance of diffusion and jumps during calm and turbulent periods.

The reminder of the paper is organized as follows. Section 2 introduces the hyper-exponential jump-diffusion model and presents our theoretical contributions regarding the pricing of European and American put options, and the early exercise jump-diffusion disentanglement. In Section 3, we present and discuss our calibration results as well as the implications for the disentanglement. Section 4 concludes the paper.

## 2. Option pricing and disentanglement in the HEJD model

### 2.1. Model formulation

We consider a filtered probability space $(\Omega, \mathcal{F}, \mathbb{F} = \{\mathcal{F}_t, t \geq 0\}, \mathbb{Q})$ satisfying the usual assumptions. The asset price dynamics under the fixed risk-neutral probability measure $\mathbb{Q}$ follows a hyper-exponential jump-diffusion process

$$\frac{dS_t}{S_{t^-}} = (r - \delta - \lambda\zeta)dt + \sigma dW_t + d\left(\sum_{i=1}^{N_t}(V_i - 1)\right), \tag{1}$$

where $\{W_t,\, t \geq 0\}$ is a standard Brownian motion under $\mathbb{Q}$. The interest rate $r \in \mathbb{R}_+$, the dividend yield $\delta \in \mathbb{R}_+$, and the volatility $\sigma \in \mathbb{R}_+$ are constants.[6] The Poisson process $\{N_t,\, t \geq 0\}$ is characterized by the jump intensity parameter $\lambda \in \mathbb{R}_+$ and $\{Y_i := \log(V_i) : i = 1, 2, \ldots\}$ is a sequence of independent and identically distributed hyper-exponential random variables with probability density function

$$\varphi_Y(y) = \sum_{i=1}^{m} p_i \eta_i e^{-\eta_i y} \mathbb{1}_{\{y \geq 0\}} + \sum_{j=1}^{n} q_j \theta_j e^{\theta_j y} \mathbb{1}_{\{y < 0\}}, \tag{2}$$

where $m, n \in \mathbb{N}$. The coefficients $p_i > 0$ for all $i = 1, \ldots, m$ and $q_j > 0$ for all $j = 1, \ldots, n$ are probabilities of different kinds of positive and negative jumps, respectively, satisfying $\sum_{i=1}^{m} p_i + \sum_{j=1}^{n} q_j = 1$. Similarly, the parameters $\eta_i > 1$ for all $i = 1, \ldots, m$ and $\theta_j > 0$ for all $j = 1, \ldots, n$ are magnitude parameters of different kinds of random upward and downward jumps, respectively. Furthermore,

[3] General properties of the HEJD model are thoroughly analyzed and discussed in Cai (2009).

[4] Jeannin and Pistorius (2010) and Crosby et al. (2010) show that any Lévy process with completely monotone Lévy density can be approximated by a HEJD process. Such Lévy models include, e.g., the Variance-Gamma, the Normal-Inverse-Gaussian, the Carr-Geman-Madan-Yor model.

[5] American option pricing in double-exponential and hyper-exponential jump-diffusion setting has been studied Kou and Wang (2004) and Cai and Sun (2014). These papers are based on the quadratic approximation of Barone-Adesi and Whaley (1987). Avram et al. (2002) consider fluctuation theory approach in a spectrally one-sided (positive or negative) Lévy model. Levendorskiĭ (2004a); 2004b) analyze regular Lévy processes of exponential type using the Wiener-Hopf factorization formula embedded in the dynamic programming approach.

[6] We remark that the assumption of positive interest rates is, under reasonable parameter specifications, not restrictive for our analysis and implementation using the Gaver–Stehfest canadization method. However, for this numerical method, we require dividends to be continuous and deterministic.

$\mathcal{F}_t = \sigma(W_s, N_s; s \le t, \{V_{j=1,\dots,N_t}\})$.[7] For ease of notation, we denote by HEJD($m$, $n$) an HEJD model with $m$ different types of positive and $n$ different types of negative jumps. The average (percentage) jump size is given by

$$\zeta := \mathbb{E}[e^{Y_1} - 1] = \sum_{i=1}^{m} \frac{p_i \eta_i}{\eta_i - 1} + \sum_{j=1}^{n} \frac{q_j \theta_j}{\theta_j + 1} - 1. \tag{3}$$

For our purpose, it is convenient to introduce the log-return process

$$X_t := \log(S_t/S_0) = \mu t + \sigma W_t + \sum_{i=1}^{N_t} Y_i, \tag{4}$$

with risk-neutral drift $\mu = r - \delta - \lambda\zeta - \frac{\sigma^2}{2}$. The log-return process has a cumulant generating function given by

$$\begin{aligned}\Psi(u) &:= \frac{1}{t}\log \mathbb{E}[e^{uX_t}] \\ &= \frac{\sigma^2}{2}u^2 + \mu u + \lambda\left(\sum_{i=1}^{m}\frac{p_i\eta_i}{\eta_i - u} + \sum_{j=1}^{n}\frac{q_j\theta_j}{\theta_j + u} - 1\right),\end{aligned} \tag{5}$$

for any $u \in (-\theta_1, \eta_1)$. Cai (2009) proved that the characteristic equation $\Psi(u) = \kappa$ for $\kappa \in \mathbb{R}_+$ has exactly $(n+m+2)$ different real roots and showed that there is no analytical solution in the general case. In fact, the only candidates of analytically tractable root-finding problems within the broad class of HEJD processes are: *a)* Pure geometric Brownian motion models, i.e., HEJD(0,0), *b)* jump-diffusions with only one type of jumps, either positive or negative, i.e., HEJD(1,0) and HEJD(0,1), or *c)* double-exponential jump-diffusion models, i.e., HEJD(1,1).[8]

### 2.2. Option pricing

Our approach is closely related to the maturity randomization method introduced in finance by Carr (1998), which has its mathematical roots in the Post-Widder inversion formula. To provide a brief sketch of the randomization method, consider an ordinary European put on the stock $S$ with strike $K$ and residual maturity, $\tau := T - t$. Under the measure $\mathbb{Q}$, the time-$t$ price of the put is

$$p(S,\tau) = \mathbb{E}\left[e^{-r\tau}(K - S_T)^+ | S_t = S\right]. \tag{6}$$

The first step of the randomization method is the derivation of so-called "Canadized" version of European and American options, where the maturity of the contract is random. To obtain the Canadized version of (6), we assume the residual maturity to be exponentially distributed with mean $\tau$, i.e., we consider the randomized residual maturity $\tilde{\tau} \sim \exp(\alpha)$, where $\alpha := \tau^{-1}$. Denoting by $p^*(S, \alpha)$ the Canadized European put value at time $t$ with random time to maturity $\tilde{\tau}$, we have

$$\begin{aligned}p^*(S,\alpha) &= \mathbb{E}\left[e^{-r\tilde{\tau}}(K - S_{t+\tilde{\tau}})^+ | S_t = S\right] \\ &= \mathbb{E}\left[\mathbb{E}\left[e^{-r\tau}(K - S_T)^+ | S_t = S, \tilde{\tau} = \tau\right]\right] \\ &= \mathbb{E}[p(S,\tilde{\tau})] = \int_0^\infty \alpha e^{-\alpha\tau} p(S,\tau)d\tau =: \mathcal{LC}(p(S,\tau)),\end{aligned} \tag{7}$$

where $\mathcal{LC}(p(S,\tau))$ is the Laplace–Carson transform of the European put price $p(S, \tau)$. Once we have calculated the Canadized version $p^*(S, \alpha)$, we can use an inversion method to determine the price of the ordinary European put price $p(S, \tau)$. While the assumption of an exponentially distributed maturity leads to simple approximations, they generate large numerical errors.[9] To improve the approximation, we instead assume that the time to maturity may be subdivided into $N$ subperiods, for which Carr (1998) assumes the Erlang-$N$ distribution. As $N \to \infty$, the Erlang distribution converges to a point mass concentrated at the mean. Hence, for large $N$, the value of an option with random maturity approximates the value of the option with the original maturity.

Contrary to Carr's randomization where the Erlangian assumption requires us to solve a time-consuming dynamic programming problem, we adopt an alternative randomization technique, which allows us to derive analytic expressions for option prices in the hyper-exponential jump-diffusion setting.[10] The original idea stems from queuing theory. Gaver (1966) introduced a three-parameter family of density functions (henceforth Gaver distribution) corresponding to the $(k_1+1)$-st smallest member of the $(k_1+k_2)$-sized sample ($k_1, k_2 \in \mathbb{N}$) of independent and identically distributed exponential random variables,

$$f_{k_1,k_2}(\tau;\nu) = \frac{(k_1+k_2)!}{k_1!(k_2-1)!}\left(1 - e^{-\nu\tau}\right)^{k_1} \nu e^{-k_2\nu\tau}, \quad \tau \ge 0. \tag{8}$$

The asymptotic convergence of a Gaver distribution to a Dirac delta function means that for a continuous function $g(\cdot)$ defined on $\mathbb{R}_+$, it holds that

$$g(\tau) = \lim_{k_1,k_2\to\infty} g^*_{k_1,k_2}, \tag{9}$$

where

$$g^*_{k_1,k_2} := \int_0^\infty f_{k_1,k_2}(\tau;\nu) g(\tau) d\tau. \tag{10}$$

Moreover, the Gaver distribution has a special computational advantage over the Erlang distribution used in Carr (1998), since the sequence of approximations $(g^*_{k_1,k_2})_{k_1,k_2\ge 1}$ satisfies the recursive relationship:

$$g^*_{0,k_2}(\nu) = \int_0^\infty g(\tau) k_2 \nu e^{-k_2\nu\tau} d\tau, \tag{11}$$

$$g^*_{k_1,k_2} = \frac{k_1+k_2}{k_1} g^*_{k_1-1,k_2} - \frac{k_2}{k_1} g^*_{k_1-1,k_2+1}. \tag{12}$$

This relationship substantially simplifies calculations, because we need to solve analytically only Eq. (11), i.e., we need to compute the analytic expression for the Laplace-Carson transform of the original function $g(\cdot)$. Therefore, if we would have analytical solutions for the Canadized options, the Gaver–Stehfest inversion algorithm in Eqs. (11) and (12) allows for an efficient computation of the original option prices.[11] The parameter $\nu$ depends on the chosen statistic of the Gaver distribution to which the sequence of random times to maturity asymptotically converges. We decide to use the mode-matching approach, i.e., $\nu := \log(2)/\tau$. Additionally, for computational convenience we consider the case $k_1 = k_2 = k \in \mathbb{N}$. Therefore, from Eqs. (7) and (11) we obtain the Laplace–Carson parameter $\alpha$ in the form $\alpha = k'\nu = k'\log(2)/\tau$, for $k' = 1, 2, \dots, 2k$. For the numerical implementation we use $k = 4$, because it provides accurate and robust numerical results in the HEJD framework. We refer to Kimura (2010) for more details.

Equipped with an efficient randomization methodology, we can address the problem of deriving Canadized variants of European

[7] Given a jump type, the magnitude parameter is the inverse of the corresponding average jump size, e.g., a magnitude parameter of 50 corresponds to the average jump of 2 percent.

[8] Including additional jump types gives rise to a mathematical problem of solving quintic, sextic, or even higher order equations which are not analytically solvable, and one has to revert to numerical procedures in such cases.

[9] See, Carr, 1998, Table 1.

[10] See, e.g., Kou and Wang, 2003; Sepp, 2004; Kimura, 2010, and Hofer and Mayer, 2013.

[11] For and overview of the Gaver–Stehfest algorithm and other Laplace inversion techiques, we refer to Valkó and Abate (2004); Abate and Whitt (2006) and Kuznetsov (2013).

and American options.[12] Indeed, we get the following result for European options. All proofs are delegated to the appendix.

**Theorem 1.** *Under the hyper-exponential jump-diffusion model (1)–(4), the price of a Canadized European put option with strike K and time to maturity $\tau$ given the underlying spot price $S_t$ is*

$$p^*(S_t,\alpha)=\begin{cases}\sum_{i=1}^{m+1}\underline{w}_i\left(\frac{S_t}{K}\right)^{\beta_{i,r+\alpha}}+\frac{\alpha K}{\alpha+r}-\frac{\alpha S_t}{\alpha+\delta} & \text{if } S_t<K,\\ \sum_{j=1}^{n+1}\overline{w}_j\left(\frac{S_t}{K}\right)^{\gamma_{j,r+\alpha}} & \text{if } S_t\geq K.\end{cases}\tag{13}$$

*The coefficients $\beta_{1,r+\alpha},\ldots,\beta_{m+1,r+\alpha}$ and $\gamma_{1,r+\alpha},\ldots,\gamma_{n+1,r+\alpha}$ are positive and negative roots of the characteristic equation $\Psi(u)=r+\alpha$. The Lévy exponent $\Psi(\cdot)$ is defined in (5) and the coefficients $\underline{w}_1,\ldots,\underline{w}_{m+1},\overline{w}_1,\ldots,\overline{w}_{n+1}$ solve the system of Eq. (36) of Appendix A.1.*

For American options, the same procedure as for European options applies. Considering the American put

$$P(S,\tau)=\operatorname{ess\,sup}_{\tau_{B_p}\in[0,T-t]}\mathbb{E}[e^{-r\tau_{B_p}}(K-S_{t+\tau_{B_p}})^+\mid S=S_t],\tag{14}$$

where $\tau_{B_p}$ is the first hitting time of the early exercise boundary $B_p$ of the process (1), we can write the Laplace–Carson transform of the American put price as

$$P^*(S,\alpha)=\mathcal{LC}(P(S,\tau)).\tag{15}$$

Hence, given an analytical expression for its Canadized variant which we present in the theorem below, we can use the Gaver–Stehfest inversion algorithm outlined above to efficiently calculate the prices of American put options with finite maturity.

**Theorem 2.** *Under the hyper-exponential jump-diffusion model (1)–(4), the price of a Canadized American put option with strike K and time to maturity $\tau$ given the underlying spot price $S_t$ is*

$$P^*(S_t,\alpha)=\begin{cases}p^*(S_t,\alpha)+e_p^*(S_t,\alpha) & \text{if } S_t>B_p^*,\\ K-S_t & \text{if } S_t\leq B_p^*,\end{cases}\tag{16}$$

*where $B_p^*$ is the time-independent early exercise boundary, $p^*(\cdot)$ is the Canadized European put option price (13), and $e_p^*(\cdot)$ is the early exercise premium given by*

$$e_p^*(S_t,\alpha)=\begin{cases}\sum_{j=1}^{n+1}\nu_j\left(\frac{S_t}{B_p^*}\right)^{\gamma_{j,r+\alpha}} & \text{if } S_t>B_p^*,\\ K-S_t-p^*(S_t,\alpha) & \text{if } S_t\leq B_p^*,\end{cases}\tag{17}$$

*using the same notation as in Theorem 1. The coefficients $\nu_1,\ldots,\nu_{n+1}$ solve the matrix Eq. (53) and the early exercise boundary $B_p^*$ can be obtained by numerically solving the Eq. (58) of Appendix A.2.*

The two theorems generalize the results of Kimura (2010), who analyzed European and American options in the Black–Scholes model. Moreover, the above result on European options generalizes Sepp (2004), who applied the same technique in the special case of a double-exponential jump-diffusion model.[13] However, we emphasize that American options have not yet been priced in a jump-diffusion setting using the Gaver–Stehfest canadization (GSC) technique outlined above.

### 2.3. Disentangling jumps and diffusion

Generally, an American option is exercised in a jump-diffusion model, if the stock price either exactly hits the early exercise boundary or the price jumps into the interior of the exercise region. Paths of the diffusion process are almost surely continuous, hence an early exercise at the boundary is due to the pure diffusion. However, conditional on stopping of the process, continuously distributed jumps will almost surely overshoot the critical price and trigger the early exercise inside of the stopping region.

Given this property, a natural question arises. Can we disentangle the contribution of jumps and diffusion on the early exercise premium of American options? By combining our adoption of the Gaver–Stehfest Canadization approach with the martingale method for option pricing and some recent results on the Laplace transform of the first hitting time to a lower flat boundary developed in Yin et al. (2013), we obtain the following result on the decomposition of the early exercise premium for the Canadized American put.

**Theorem 3.** *In the continuation region, the early exercise premium for the Canadized American put can be orthogonally decomposed as*

$$e_p^*(S_t,\alpha)=e_{p,d}^*(S_t,\alpha)+e_{p,j}^*(S_t,\alpha),\tag{18}$$

*where $e_{p,d}^*(S_t,\alpha)$ represents the fraction of the early exercise premium due to the diffusion of the process, and $e_{p,j}^*(S_t,\alpha)$ is the contribution of jumps to the early exercise premium. The overall contribution of jumps can be further orthogonally decomposed into components associated with each type of negative jumps, i.e.,*

$$e_{p,j}^*(S_t,\alpha)=\sum_{l=1}^{n}e_{p,j,l}^*(S_t,\alpha),\tag{19}$$

*where $e_{p,j,l}^*(S_t,\alpha)$ corresponds to the negative jump of kind $l=1,2,\ldots,n$. Analytic expressions for the diffusion and jump components are given in (68) and (70) of Appendix A.3.*

Given the above result for the Canadized American options, we can invert the Laplace–Carson transform to obtain the early exercise premium disentanglement in the original space.

### 2.4. Numerical examples

To demonstrate the pricing accuracy of the GSC method in a HEJD model, we compute European and American put option prices and benchmark the results against the Fourier space time-stepping technique (FST) of Jackson et al. (2008).[14] In particular, European option prices are obtained using a grid of 65,536 points and American option prices are computed using the 4-step Richardson extrapolation based on (four) Bermudan option prices with 16,384 space steps each, and 256, 512, 1,024, and 2048 time steps, respectively. Furthermore, we report numerical results for the GSC method that relies on the mode-matching approach with a 4-step recursive scheme.

We assume that the current underlying asset price is 100, the risk-free rate is 4 percent, and the dividend yield is 2 percent. Without loss of generality, we focus on the double-exponential jump-diffusion model of Kou (2002), i.e., HEJD(1,1). The volatility is set to either 15 or 30 percent, the jump intensity takes values of either 5 or 10 (jumps per annum), the conditional probability of a negative jump is fixed at 70 percent, the positive jump parameter (average positive jump size) is either 100 (1 percent) or 200 (0.5 percent), and the negative jump parameter (average negative jump size) is either 25 (4 percent) or 50 (2 percent). We compute prices of OTM and ATM European and American put options, because these are most frequently traded options in the market. The

[12] Note that we only give the results for put options. The corresponding values for call options follow from the symmetry relation of Schroder (1999).

[13] Sepp (2004) considers pricing of European-style vanilla and barrier options in a double-exponential jump-diffusion model.

[14] For pricing American options in the HEJD framework our numerical tests, which we do not report here, suggest that the FST exhibits superior speed-accuracy characteristics than the convolution method of Lord (2008) and the cosine method of Fang and Oosterlee (2009).

**Table 1**
Pricing performance of the Gaver-Stehfest canadization method (GSC) for OTM and ATM put options with time to maturity $\tau = 3$ months. European and American put option prices are computed via the GSC method for a range of double-exponential jump-diffusion models. The underlying asset price is set to $S_t = 100$, the risk-free rate is $r = 0.04$, the dividend yield is fixed at $\delta = 0.02$, and the conditional probability of a negative jump is $q = 0.7$. Variable input parameters are strike, volatility $\sigma$, jump intensity $\lambda$, positive jump parameter $\eta$, and negative jump parameter $\theta$. We compare the results of our approach to the benchmark (Fourier space time-stepping method), and report the relative pricing errors in percentages.

| | Parameters | | | | Benchmark | | GSC Method | | Rel. Error (%) | |
|---|---|---|---|---|---|---|---|---|---|---|
| Strike | $\sigma$ | $\lambda$ | $\eta$ | $\theta$ | European | American | European | American | European | American |
| 100 | 0.15 | 5 | 100 | 25 | 3.3150 | 3.3642 | 3.3150 | 3.3409 | −0.0006 | −0.6933 |
| 100 | 0.15 | 5 | 100 | 50 | 2.9135 | 2.9559 | 2.9135 | 2.9333 | −0.0004 | −0.7676 |
| 100 | 0.15 | 5 | 200 | 25 | 3.3027 | 3.3523 | 3.3026 | 3.3288 | −0.0006 | −0.7025 |
| 100 | 0.15 | 5 | 200 | 50 | 2.8997 | 2.9426 | 2.8997 | 2.9196 | −0.0005 | −0.7802 |
| 100 | 0.15 | 10 | 100 | 25 | 3.8487 | 3.9041 | 3.8486 | 3.8780 | −0.0017 | −0.6688 |
| 100 | 0.15 | 10 | 100 | 50 | 3.0910 | 3.1350 | 3.0910 | 3.1116 | −0.0004 | −0.7447 |
| 100 | 0.15 | 10 | 200 | 25 | 3.8274 | 3.8836 | 3.8273 | 3.8571 | −0.0017 | −0.6837 |
| 100 | 0.15 | 10 | 200 | 50 | 3.0648 | 3.1097 | 3.0648 | 3.0858 | −0.0004 | −0.7673 |
| 100 | 0.30 | 5 | 100 | 25 | 6.0219 | 6.0650 | 6.0219 | 6.0379 | 0.0003 | −0.4467 |
| 100 | 0.30 | 5 | 100 | 50 | 5.7865 | 5.8272 | 5.7865 | 5.8010 | 0.0004 | −0.4497 |
| 100 | 0.30 | 5 | 200 | 25 | 6.0148 | 6.0579 | 6.0148 | 6.0308 | 0.0003 | −0.4480 |
| 100 | 0.30 | 5 | 200 | 50 | 5.7792 | 5.8199 | 5.7792 | 5.7937 | 0.0004 | −0.4510 |
| 100 | 0.30 | 10 | 100 | 25 | 6.3415 | 6.3871 | 6.3415 | 6.3588 | 0.0003 | −0.4430 |
| 100 | 0.30 | 10 | 100 | 50 | 5.8825 | 5.9237 | 5.8826 | 5.8972 | 0.0004 | −0.4471 |
| 100 | 0.30 | 10 | 200 | 25 | 6.3280 | 6.3737 | 6.3280 | 6.3453 | 0.0003 | −0.4453 |
| 100 | 0.30 | 10 | 200 | 50 | 5.8681 | 5.9094 | 5.8681 | 5.8828 | 0.0004 | −0.4497 |
| 95 | 0.15 | 5 | 100 | 25 | 1.5092 | 1.5284 | 1.5093 | 1.5195 | 0.0075 | −0.5804 |
| 95 | 0.15 | 5 | 100 | 50 | 1.1098 | 1.1220 | 1.1099 | 1.1152 | 0.0109 | −0.6108 |
| 95 | 0.15 | 5 | 200 | 25 | 1.5009 | 1.5202 | 1.5010 | 1.5113 | 0.0076 | −0.5897 |
| 95 | 0.15 | 5 | 200 | 50 | 1.1004 | 1.1128 | 1.1005 | 1.1058 | 0.0113 | −0.6243 |
| 95 | 0.15 | 10 | 100 | 25 | 1.9942 | 2.0196 | 1.9943 | 2.0078 | 0.0048 | −0.5847 |
| 95 | 0.15 | 10 | 100 | 50 | 1.2614 | 1.2754 | 1.2615 | 1.2677 | 0.0090 | −0.6036 |
| 95 | 0.15 | 10 | 200 | 25 | 1.9792 | 2.0050 | 1.9793 | 1.9930 | 0.0050 | −0.5998 |
| 95 | 0.15 | 10 | 200 | 50 | 1.2432 | 1.2575 | 1.2433 | 1.2496 | 0.0094 | −0.6275 |
| 95 | 0.30 | 5 | 100 | 25 | 3.7908 | 3.8142 | 3.7908 | 3.7991 | 0.0013 | −0.3966 |
| 95 | 0.30 | 5 | 100 | 50 | 3.5565 | 3.5777 | 3.5566 | 3.5636 | 0.0014 | −0.3945 |
| 95 | 0.30 | 5 | 200 | 25 | 3.7845 | 3.8080 | 3.7845 | 3.7928 | 0.0013 | −0.3979 |
| 95 | 0.30 | 5 | 200 | 50 | 3.5500 | 3.5713 | 3.5500 | 3.5571 | 0.0014 | −0.3959 |
| 95 | 0.30 | 10 | 100 | 25 | 4.1014 | 4.1273 | 4.1014 | 4.1109 | 0.0012 | −0.3974 |
| 95 | 0.30 | 10 | 100 | 50 | 3.6471 | 3.6689 | 3.6472 | 3.6544 | 0.0013 | −0.3934 |
| 95 | 0.30 | 10 | 200 | 25 | 4.0894 | 4.1154 | 4.0895 | 4.0990 | 0.0012 | −0.3997 |
| 95 | 0.30 | 10 | 200 | 50 | 3.6343 | 3.6561 | 3.6343 | 3.6416 | 0.0013 | −0.3960 |
| 90 | 0.15 | 5 | 100 | 25 | 0.5920 | 0.5988 | 0.5926 | 0.5963 | 0.1110 | −0.4103 |
| 90 | 0.15 | 5 | 100 | 50 | 0.3080 | 0.3107 | 0.3087 | 0.3098 | 0.2196 | −0.2952 |
| 90 | 0.15 | 5 | 200 | 25 | 0.5879 | 0.5947 | 0.5885 | 0.5922 | 0.1106 | −0.4204 |
| 90 | 0.15 | 5 | 200 | 50 | 0.3039 | 0.3067 | 0.3046 | 0.3057 | 0.2193 | −0.3104 |
| 90 | 0.15 | 10 | 100 | 25 | 0.9285 | 0.9392 | 0.9291 | 0.9348 | 0.0690 | −0.4634 |
| 90 | 0.15 | 10 | 100 | 50 | 0.3951 | 0.3987 | 0.3958 | 0.3973 | 0.1749 | −0.3401 |
| 90 | 0.15 | 10 | 200 | 25 | 0.9199 | 0.9308 | 0.9205 | 0.9263 | 0.0687 | −0.4793 |
| 90 | 0.15 | 10 | 200 | 50 | 0.3865 | 0.3902 | 0.3872 | 0.3887 | 0.1746 | −0.3665 |
| 90 | 0.30 | 5 | 100 | 25 | 2.1808 | 2.1925 | 2.1811 | 2.1851 | 0.0142 | −0.3408 |
| 90 | 0.30 | 5 | 100 | 50 | 1.9723 | 1.9823 | 1.9726 | 1.9757 | 0.0161 | −0.3321 |
| 90 | 0.30 | 5 | 200 | 25 | 2.1759 | 2.1876 | 2.1762 | 2.1801 | 0.0143 | −0.3421 |
| 90 | 0.30 | 5 | 200 | 50 | 1.9672 | 1.9772 | 1.9675 | 1.9706 | 0.0162 | −0.3334 |
| 90 | 0.30 | 10 | 100 | 25 | 2.4525 | 2.4662 | 2.4528 | 2.4576 | 0.0120 | −0.3476 |
| 90 | 0.30 | 10 | 100 | 50 | 2.0480 | 2.0584 | 2.0483 | 2.0515 | 0.0152 | −0.3330 |
| 90 | 0.30 | 10 | 200 | 25 | 2.4430 | 2.4567 | 2.4433 | 2.4482 | 0.0121 | −0.3499 |
| 90 | 0.30 | 10 | 200 | 50 | 2.0379 | 2.0483 | 2.0382 | 2.0415 | 0.0154 | −0.3355 |

performance of the GSC method is measured by the relative pricing error with respect to the benchmark method (FST).

Table 1 provides results for options with 3 months to maturity. Table 2 summarizes the results for options with 1 year to maturity. We conclude that European options are accurately priced with the GSC method in all cases, with absolute relative error not exceeding 0.3 percent, and being less than 0.001 percent in many cases. On the other hand, American options have larger absolute relative errors, which are in the range between 0.2 and 1.4 percent. However, American options with shorter time to maturity, i.e., 3 months, are more accurately priced. This is important because jump-diffusion dynamics are generally plausible for pricing of short term options, and our example demonstrates that GSC method performs well for such options. The absolute relative error increases with moneyness and varies between 0.3 and 0.8 percent for ATM options, and between 0.2 and 0.5 percent for OTM options. These errors are lower than the typically observed bid-ask spread for ATM and OTM options. Hence, we conclude that the proposed method works well.

Next, we compute the contribution of diffusion and jump components to the early exercise premium for OTM and ATM American put options. Table 3 summarizes our disentanglement results for options with 3 months and 1 year maturity. Early exercise premium, expressed as a percentage of the American put option, increases with moneyness and time to maturity and varies between 0.1 and 2.7 percent. The contribution of jumps can be as low as 3 percent or as high as 66 percent of the early exercise premium, depending on the model and the option contract.

**Table 2**
Pricing performance of the Gaver-Stehfest canadization method (GSC) for OTM and ATM put options with time to maturity $\tau = 1$ year. European and American put option prices are computed via the GSC method for a range of double-exponential jump-diffusion models. The underlying asset price is set to $S_t = 100$, the risk-free rate is $r = 0.04$, the dividend yield is fixed at $\delta = 0.02$, and the conditional probability of a negative jump is $q = 0.7$. Variable input parameters are strike, volatility $\sigma$, jump intensity $\lambda$, positive jump parameter $\eta$, and negative jump parameter $\theta$. We compare the results of our approach to the benchmark (Fourier space time-stepping method), and report the relative pricing errors in percentages.

| | Parameters | | | | Benchmark | | GSC Method | | Rel. Error (%) | |
|---|---|---|---|---|---|---|---|---|---|---|
| Strike | $\sigma$ | $\lambda$ | $\eta$ | $\theta$ | European | American | European | American | European | American |
| 100 | 0.15 | 5 | 100 | 25 | 6.1209 | 6.3733 | 6.1209 | 6.2888 | −0.0007 | −1.3273 |
| 100 | 0.15 | 5 | 100 | 50 | 5.2566 | 5.4783 | 5.2566 | 5.4025 | −0.0005 | −1.3834 |
| 100 | 0.15 | 5 | 200 | 25 | 6.0972 | 6.3504 | 6.0972 | 6.2656 | −0.0008 | −1.3347 |
| 100 | 0.15 | 5 | 200 | 50 | 5.2295 | 5.4519 | 5.2295 | 5.3759 | −0.0005 | −1.3927 |
| 100 | 0.15 | 10 | 100 | 25 | 7.1837 | 7.4587 | 7.1837 | 7.3620 | −0.0005 | −1.2970 |
| 100 | 0.15 | 10 | 100 | 50 | 5.6092 | 5.8374 | 5.6092 | 5.7581 | −0.0005 | −1.3583 |
| 100 | 0.15 | 10 | 200 | 25 | 7.1426 | 7.4190 | 7.1426 | 7.3219 | −0.0005 | −1.3097 |
| 100 | 0.15 | 10 | 200 | 50 | 5.5579 | 5.7873 | 5.5579 | 5.7077 | −0.0005 | −1.3752 |
| 100 | 0.30 | 5 | 100 | 25 | 11.2944 | 11.5435 | 11.2943 | 11.4378 | −0.0007 | −0.9154 |
| 100 | 0.30 | 5 | 100 | 50 | 10.8175 | 11.0562 | 10.8175 | 10.9545 | −0.0006 | −0.9205 |
| 100 | 0.30 | 5 | 200 | 25 | 11.2806 | 11.5298 | 11.2806 | 11.4242 | −0.0007 | −0.9165 |
| 100 | 0.30 | 5 | 200 | 50 | 10.8033 | 11.0420 | 10.8032 | 10.9402 | −0.0006 | −0.9217 |
| 100 | 0.30 | 10 | 100 | 25 | 11.9280 | 12.1881 | 11.9279 | 12.0777 | −0.0007 | −0.9061 |
| 100 | 0.30 | 10 | 100 | 50 | 11.0052 | 11.2462 | 11.0051 | 11.1432 | −0.0006 | −0.9155 |
| 100 | 0.30 | 10 | 200 | 25 | 11.9019 | 12.1622 | 11.9018 | 12.0517 | −0.0007 | −0.9083 |
| 100 | 0.30 | 10 | 200 | 50 | 10.9771 | 11.2182 | 10.9770 | 11.1152 | −0.0006 | −0.9179 |
| 95 | 0.15 | 5 | 100 | 25 | 4.0802 | 4.2299 | 4.0802 | 4.1776 | −0.0002 | −1.2372 |
| 95 | 0.15 | 5 | 100 | 50 | 3.2533 | 3.3699 | 3.2533 | 3.3271 | 0.0001 | −1.2710 |
| 95 | 0.15 | 5 | 200 | 25 | 4.0597 | 4.2096 | 4.0597 | 4.1572 | −0.0001 | −1.2448 |
| 95 | 0.15 | 5 | 200 | 50 | 3.2300 | 3.3467 | 3.2300 | 3.3038 | 0.0001 | −1.2805 |
| 95 | 0.15 | 10 | 100 | 25 | 5.0751 | 5.2516 | 5.0751 | 5.1874 | −0.0002 | −1.2223 |
| 95 | 0.15 | 10 | 100 | 50 | 3.5764 | 3.7017 | 3.5764 | 3.6552 | −0.0000 | −1.2540 |
| 95 | 0.15 | 10 | 200 | 25 | 5.0388 | 5.2160 | 5.0388 | 5.1516 | −0.0002 | −1.2351 |
| 95 | 0.15 | 10 | 200 | 50 | 3.5317 | 3.6573 | 3.5317 | 3.6108 | 0.0000 | −1.2713 |
| 95 | 0.30 | 5 | 100 | 25 | 8.8743 | 9.0538 | 8.8743 | 8.9752 | −0.0006 | −0.8685 |
| 95 | 0.30 | 5 | 100 | 50 | 8.4104 | 8.5794 | 8.4104 | 8.5047 | −0.0006 | −0.8704 |
| 95 | 0.30 | 5 | 200 | 25 | 8.8614 | 9.0409 | 8.8613 | 8.9622 | −0.0006 | −0.8697 |
| 95 | 0.30 | 5 | 200 | 50 | 8.3970 | 8.5659 | 8.3969 | 8.4912 | −0.0005 | −0.8716 |
| 95 | 0.30 | 10 | 100 | 25 | 9.4870 | 9.6780 | 9.4870 | 9.5945 | −0.0006 | −0.8628 |
| 95 | 0.30 | 10 | 100 | 50 | 8.5904 | 8.7620 | 8.5903 | 8.6861 | −0.0006 | −0.8666 |
| 95 | 0.30 | 10 | 200 | 25 | 9.4624 | 9.6534 | 9.4624 | 9.5699 | −0.0006 | −0.8650 |
| 95 | 0.30 | 10 | 200 | 50 | 8.5638 | 8.7354 | 8.5638 | 8.6595 | −0.0006 | −0.8689 |
| 90 | 0.15 | 5 | 100 | 25 | 2.5507 | 2.6343 | 2.5509 | 2.6041 | 0.0079 | −1.1443 |
| 90 | 0.15 | 5 | 100 | 50 | 1.8318 | 1.8876 | 1.8320 | 1.8659 | 0.0132 | −1.1507 |
| 90 | 0.15 | 5 | 200 | 25 | 2.5344 | 2.6180 | 2.5346 | 2.5879 | 0.0081 | −1.1519 |
| 90 | 0.15 | 5 | 200 | 50 | 1.8139 | 1.8696 | 1.8141 | 1.8479 | 0.0136 | −1.1602 |
| 90 | 0.15 | 10 | 100 | 25 | 3.4151 | 3.5232 | 3.4152 | 3.4828 | 0.0044 | −1.1463 |
| 90 | 0.15 | 10 | 100 | 50 | 2.0974 | 2.1608 | 2.0977 | 2.1361 | 0.0101 | −1.1442 |
| 90 | 0.15 | 10 | 200 | 25 | 3.3851 | 3.4935 | 3.3853 | 3.4530 | 0.0046 | −1.1591 |
| 90 | 0.15 | 10 | 200 | 50 | 2.0624 | 2.1257 | 2.0627 | 2.1011 | 0.0107 | −1.1614 |
| 90 | 0.30 | 5 | 100 | 25 | 6.7698 | 6.8951 | 6.7698 | 6.8385 | −0.0002 | −0.8217 |
| 90 | 0.30 | 5 | 100 | 50 | 6.3321 | 6.4476 | 6.3321 | 6.3947 | −0.0001 | −0.8203 |
| 90 | 0.30 | 5 | 200 | 25 | 6.7580 | 6.8832 | 6.7580 | 6.8266 | −0.0002 | −0.8228 |
| 90 | 0.30 | 5 | 200 | 50 | 6.3198 | 6.4352 | 6.3198 | 6.3824 | −0.0001 | −0.8214 |
| 90 | 0.30 | 10 | 100 | 25 | 7.3458 | 7.4820 | 7.3457 | 7.4207 | −0.0003 | −0.8196 |
| 90 | 0.30 | 10 | 100 | 50 | 6.4992 | 6.6173 | 6.4992 | 6.5632 | −0.0001 | −0.8176 |
| 90 | 0.30 | 10 | 200 | 25 | 7.3232 | 7.4594 | 7.3232 | 7.3981 | −0.0002 | −0.8216 |
| 90 | 0.30 | 10 | 200 | 50 | 6.4749 | 6.5929 | 6.4749 | 6.5389 | −0.0001 | −0.8198 |

From Table 3 we see that the diffusion (jump) contribution increases (decreases) in strike. Intuitively, this observation makes sense, since the probability that early exercise occurs due to the diffusion decreases for options that are deeper OTM. The jump contribution also increases with jump intensity and average negative jump size, while it decreases with volatility. The effect of average positive jump size on the jump contribution is negative but negligible.

## 3. Empirical analysis

We next explore empirically the disentanglement of jumps from diffusion for the early exercise premium. By calibrating different HEJD models to American options on the S&P 100 index, we analyze whether jumps play an important role for the early exercise of American put options.

### 3.1. Data and calibration procedure

We use six years of weekly (Wednesdays) S&P 100 index American options data (ticker symbol OEX), spanning the period from January 3, 2007 until December 31, 2012. Thus, the sample encompasses the recent financial crisis.[15] Since we are interested in the calibration of a jump-diffusion model, we focus on short-term op-

[15] S&P 100 index quotes, American options data (bid and ask prices, strikes and maturities), zero-coupon curve, and dividend yields are obtained from OptionMetrics.

**Table 3**
Early exercise disentanglement of jumps from diffusion for OTM and ATM American put options. We compute early exercise disentanglement for options with $\tau = 3$ months and $\tau = 1$ year to maturity for a range of double-exponential jump-diffusion models. Early exercise premium (EEP) is represented as a percentage of the American put option price. Contributions of the diffusion component (DC) and the jump component (JC) to the early exercise are represented as percentages of the EEP, hence summing up to unity. The underlying asset price is set to $S_t = 100$, the risk-free rate is $r = 0.04$, the dividend yield is fixed at $\delta = 0.02$, and the conditional probability of a negative jump is $q = 0.7$. Variable input parameters are strike, volatility $\sigma$, jump intensity $\lambda$, positive jump parameter $\eta$, and negative jump parameter $\theta$.

| | Parameters | | | | $\tau = 3$ months | | | $\tau = 1$ year | | |
|---|---|---|---|---|---|---|---|---|---|---|
| Strike | $\sigma$ | $\lambda$ | $\eta$ | $\theta$ | EEP (%) | DC (%) | JC(%) | EEP(%) | DC(%) | JC(%) |
| 100 | 0.15 | 5 | 100 | 25 | 0.78 | 48.64 | 51.36 | 2.67 | 57.73 | 42.27 |
| 100 | 0.15 | 5 | 100 | 50 | 0.67 | 83.45 | 16.55 | 2.70 | 86.43 | 13.57 |
| 100 | 0.15 | 5 | 200 | 25 | 0.79 | 48.45 | 51.55 | 2.69 | 57.54 | 42.46 |
| 100 | 0.15 | 5 | 200 | 50 | 0.68 | 83.36 | 16.64 | 2.72 | 86.35 | 13.65 |
| 100 | 0.15 | 10 | 100 | 25 | 0.76 | 35.24 | 64.76 | 2.42 | 42.53 | 57.47 |
| 100 | 0.15 | 10 | 100 | 50 | 0.66 | 72.55 | 27.45 | 2.59 | 76.56 | 23.44 |
| 100 | 0.15 | 10 | 200 | 25 | 0.77 | 34.94 | 65.06 | 2.45 | 42.20 | 57.80 |
| 100 | 0.15 | 10 | 200 | 50 | 0.68 | 72.30 | 27.70 | 2.63 | 76.33 | 23.67 |
| 100 | 0.30 | 5 | 100 | 25 | 0.26 | 83.77 | 16.23 | 1.26 | 86.81 | 13.19 |
| 100 | 0.30 | 5 | 100 | 50 | 0.25 | 96.25 | 3.75 | 1.25 | 96.66 | 3.34 |
| 100 | 0.30 | 5 | 200 | 25 | 0.27 | 83.76 | 16.24 | 1.26 | 86.79 | 13.21 |
| 100 | 0.30 | 5 | 200 | 50 | 0.25 | 96.24 | 3.76 | 1.25 | 96.65 | 3.35 |
| 100 | 0.30 | 10 | 100 | 25 | 0.27 | 73.00 | 27.00 | 1.24 | 77.01 | 22.99 |
| 100 | 0.30 | 10 | 100 | 50 | 0.25 | 92.81 | 7.19 | 1.24 | 93.56 | 6.44 |
| 100 | 0.30 | 10 | 200 | 25 | 0.27 | 72.92 | 27.08 | 1.24 | 76.94 | 23.06 |
| 100 | 0.30 | 10 | 200 | 50 | 0.25 | 92.79 | 7.21 | 1.24 | 93.54 | 6.46 |
| 95 | 0.15 | 5 | 100 | 25 | 0.67 | 46.15 | 53.85 | 2.33 | 57.14 | 42.86 |
| 95 | 0.15 | 5 | 100 | 50 | 0.48 | 82.18 | 17.82 | 2.22 | 86.18 | 13.82 |
| 95 | 0.15 | 5 | 200 | 25 | 0.68 | 45.96 | 54.04 | 2.35 | 56.95 | 43.05 |
| 95 | 0.15 | 5 | 200 | 50 | 0.48 | 82.08 | 17.92 | 2.24 | 86.10 | 13.90 |
| 95 | 0.15 | 10 | 100 | 25 | 0.67 | 34.29 | 65.71 | 2.17 | 42.10 | 57.90 |
| 95 | 0.15 | 10 | 100 | 50 | 0.49 | 71.14 | 28.86 | 2.16 | 76.23 | 23.77 |
| 95 | 0.15 | 10 | 200 | 25 | 0.68 | 34.00 | 66.00 | 2.19 | 41.77 | 58.23 |
| 95 | 0.15 | 10 | 200 | 50 | 0.51 | 70.89 | 29.11 | 2.19 | 76.00 | 24.00 |
| 95 | 0.30 | 5 | 100 | 25 | 0.22 | 83.22 | 16.78 | 1.12 | 86.69 | 13.31 |
| 95 | 0.30 | 5 | 100 | 50 | 0.20 | 96.16 | 3.84 | 1.11 | 96.64 | 3.36 |
| 95 | 0.30 | 5 | 200 | 25 | 0.22 | 83.19 | 16.81 | 1.13 | 86.67 | 13.33 |
| 95 | 0.30 | 5 | 200 | 50 | 0.20 | 96.15 | 3.85 | 1.11 | 96.63 | 3.37 |
| 95 | 0.30 | 10 | 100 | 25 | 0.23 | 72.30 | 27.70 | 1.12 | 76.85 | 23.15 |
| 95 | 0.30 | 10 | 100 | 50 | 0.20 | 92.66 | 7.34 | 1.10 | 93.52 | 6.48 |
| 95 | 0.30 | 10 | 200 | 25 | 0.23 | 72.21 | 27.79 | 1.12 | 76.78 | 23.22 |
| 95 | 0.30 | 10 | 200 | 50 | 0.20 | 92.63 | 7.37 | 1.10 | 93.50 | 6.50 |
| 90 | 0.15 | 5 | 100 | 25 | 0.62 | 43.82 | 56.18 | 2.04 | 56.46 | 43.54 |
| 90 | 0.15 | 5 | 100 | 50 | 0.35 | 80.41 | 19.59 | 1.82 | 85.89 | 14.11 |
| 90 | 0.15 | 5 | 200 | 25 | 0.62 | 43.64 | 56.36 | 2.06 | 56.26 | 43.74 |
| 90 | 0.15 | 5 | 200 | 50 | 0.36 | 80.29 | 19.71 | 1.83 | 85.81 | 14.19 |
| 90 | 0.15 | 10 | 100 | 25 | 0.61 | 33.21 | 66.79 | 1.94 | 41.64 | 58.36 |
| 90 | 0.15 | 10 | 100 | 50 | 0.38 | 69.43 | 30.57 | 1.80 | 75.87 | 24.13 |
| 90 | 0.15 | 10 | 200 | 25 | 0.62 | 32.94 | 67.06 | 1.96 | 41.31 | 58.69 |
| 90 | 0.15 | 10 | 200 | 50 | 0.39 | 69.16 | 30.84 | 1.83 | 75.63 | 24.37 |
| 90 | 0.30 | 5 | 100 | 25 | 0.18 | 82.49 | 17.51 | 1.00 | 86.56 | 13.44 |
| 90 | 0.30 | 5 | 100 | 50 | 0.16 | 96.06 | 3.94 | 0.98 | 96.62 | 3.38 |
| 90 | 0.30 | 5 | 200 | 25 | 0.18 | 82.45 | 17.55 | 1.00 | 86.54 | 13.46 |
| 90 | 0.30 | 5 | 200 | 50 | 0.16 | 96.05 | 3.95 | 0.98 | 96.61 | 3.39 |
| 90 | 0.30 | 10 | 100 | 25 | 0.20 | 71.50 | 28.50 | 1.01 | 76.68 | 23.32 |
| 90 | 0.30 | 10 | 100 | 50 | 0.16 | 92.48 | 7.52 | 0.98 | 93.49 | 6.51 |
| 90 | 0.30 | 10 | 200 | 25 | 0.20 | 71.41 | 28.59 | 1.01 | 76.61 | 23.39 |
| 90 | 0.30 | 10 | 200 | 50 | 0.16 | 92.46 | 7.54 | 0.98 | 93.47 | 6.53 |

tions with less than 60 days to maturity. We define moneyness $M$ as the ratio of the strike $K$ and the futures price $F_{t,T} := S_t e^{(r-\delta)(T-t)}$, i.e., $M := K/F_{t,T}$.

We eliminate illiquid in-the-money options (ITM), i.e., calls with moneyness less than 0.97 and puts with moneyness greater than 1.03. Hence, our sample contains only liquid near-the-money (NTM) and out-of-the-money (OTM) options. We use mid-prices, which are computed as averages of the bid and ask market quotes, as a proxy for our market prices. We also eliminate all the options whose prices are lower than 0.125 units due to the minimum tick limitations. Finally, we eliminate all the options for which the volume or the open interest are zero.

Descriptive statistics of our sample of options are given in Table 4. The total number of options in the dataset is 23,169 distributed over 313 days, or approximately 74 option quotes per observation day on average. NTM options, i.e., options for which $M \in (0.97, 1.03)$, include both calls and puts, and they account for almost 43 percent of the sample. OTM puts ($M < 0.97$) constitute around 38 percent of the dataset, and OTM calls ($M > 1.03$) account for the remaining 19 percent of all considered option quotes.

We re-calibrate parameters of a HEJD($m$, $n$) model for each observation date in the sample by minimizing a loss function in the form of penalized weighted non-linear least squares (WNLLS).

**Table 4**
S&P 100 index options data, January 3, 2007–December 31, 2012. We report descriptive statistics of ATM and OTM American options on the S&P 100 index. The data is obtained from OptionMetrics and filtered as described in the Section 3.1. The dataset comprises closing quotes for call and put options traded on Wednesdays for the given time period. There are 313 days of observations in total. We report the number of option contracts traded, the average quoted price and the average implied volatility. Each statistic is computed for four different maturity bins and six different moneyness bins, as well as for collective observations across given maturity and moneyness buckets. DTM stands for days-to-maturity, and $M := K/F_{t,T}$ denotes moneyness.

Panel A: Number of contracts across moneyness and maturity

| Moneyness | DTM < 7 | 7 ≤ DTM < 14 | 14 ≤ DTM < 30 | 30 ≤ DTM < 60 | All |
|---|---|---|---|---|---|
| M < 0.94 | 271 | 593 | 1842 | 3902 | 6608 |
| 0.94<M<0.97 | 525 | 244 | 485 | 1002 | 2256 |
| 0.97<M<1.00 | 1702 | 494 | 964 | 1921 | 5081 |
| 1.00<M<1.03 | 1476 | 480 | 958 | 1909 | 4823 |
| 1.03<M<1.06 | 177 | 188 | 453 | 1011 | 1829 |
| 1.06<M | 84 | 150 | 513 | 1,825 | 2,572 |
| All | 4235 | 2149 | 5215 | 11,570 | 23,169 |

Panel B: Average quoted price across moneyness and maturity

| Moneyness | DTM < 7 | 7 ≤ DTM < 14 | 14 ≤ DTM < 30 | 30 ≤ DTM < 60 | All |
|---|---|---|---|---|---|
| M < 0.94 | 0.39 | 0.68 | 1.19 | 2.92 | 2.14 |
| 0.94<M<0.97 | 0.54 | 1.83 | 3.76 | 7.70 | 4.55 |
| 0.97<M<1.00 | 5.02 | 8.75 | 11.50 | 15.79 | 10.69 |
| 1.00<M<1.03 | 5.04 | 7.93 | 10.52 | 14.48 | 10.15 |
| 1.03<M<1.06 | 0.66 | 1.24 | 1.97 | 4.73 | 3.30 |
| 1.06<M | 0.58 | 0.82 | 0.92 | 2.00 | 1.67 |
| All | 3.91 | 4.35 | 5.09 | 7.39 | 5.96 |

Panel C: Average implied volatility across moneyness and maturity

| Moneyness | DTM < 7 | 7 ≤ DTM < 14 | 14 ≤ DTM < 30 | 30 ≤ DTM < 60 | All |
|---|---|---|---|---|---|
| M < 0.94 | 0.8058 | 0.4177 | 0.3734 | 0.3384 | 0.3745 |
| 0.94<M<0.97 | 0.4866 | 0.2681 | 0.2439 | 0.2359 | 0.2991 |
| 0.97<M<1.00 | 0.3385 | 0.2294 | 0.2145 | 0.2128 | 0.2557 |
| 1.00<M<1.03 | 0.3141 | 0.2058 | 0.1924 | 0.1944 | 0.2307 |
| 1.03<M<1.06 | 0.4682 | 0.2138 | 0.1760 | 0.1745 | 0.2073 |
| 1.06<M | 0.9103 | 0.4012 | 0.2554 | 0.2196 | 0.2600 |
| All | 0.3971 | 0.2912 | 0.2700 | 0.2519 | 0.2855 |

In particular, we consider a weighted Euclidian distance between market quotes and corresponding model option prices.[16] Nevertheless, it is well known that any framework involving re-calibration of the model parameters inherently suffers from instability and the non-convexity of the multidimensional loss function implies the existence of local minima. Therefore, we add a positive and locally convex penalty term to the loss function and recast the original problem into a sequential regularized weighted non-linear least squares setting. We follow Hellmich et al. (2013) and define the penalty function as the Kulback–Leibler divergence between the probability distributions on two successive points in time.[17] The probability density function of the HEJD process is not known in closed form, but we are able to numerically compute the Kullback–Leibler divergence by using the Fourier cosine method of Fang and Oosterlee (2004).[18]

### 3.2. Model selection

The HEJD($m$, $n$) offers the flexibility to choose any number of distinct positive and negative jump types. To keep the analysis tractable, we consider a set of HEJD($m$, $n$) models for which the total number of different jump types is such that $m+n \leq 4$, which gives us 15 different models with up to nine parameters.[19] This choice includes some special cases such as, e.g., HEJD(0, 0) is the no-jump case of Black and Scholes (1973), HEJD(1, 1) is the double-exponential model of Kou (2002), and HEJD(0, 1) is the spectrally one-sided (negative) exponential Lévy model of Avram et al. (2002).

Given the Bayesian nature of the sequential regularized WNLLS procedure due to the penalty function, we can transform our calibration exercise into a series of maximum a posteriori problems (MAP), which can be considered as a regularized maximum likelihood approach.[20] In addition to the MAP objective function,

[16] We follow Lindström et al. (2008) and define the weights as the inverse of the squared bid-ask spreads.

[17] Others, like Cont and Tankov (2004), opt for the relative entropy as an alternative to ensure positivity. However, the relative entropy approach is based on the Kullback-Leibler divergence with respect to the prior model on the path space. It implies that the volatility parameter would remain constant in order to have non-singular (equivalent) probabilities. In fact, the choice of the penalty term defined as the relative entropy function would make it impossible to obtain dynamic diffusion parameters.

[18] A detailed description of the calibration procedure can be obtained from the authors.

[19] Further in text, we use interchangeably the notation HEJD($m$, $n$) and ($m$, $n$). We also note that it is necessary to introduce a constraint on the total number of different positive and negative jump types in the model. Generally, the HEJD class of models admits a (countably) infinite number of jumps. However, in practical applications we have to limit the number of parameters to keep our analysis tractable and to avoid overfitting. Our particular choice of $m+n \leq 4$ is motivated by two facts. First, this set contains the most popular HEJD model specifications which are studied in the literature. Second, the total number of calibration parameters when $n+m=4$ is nine, which is already quite high for a single-asset option pricing model.

[20] The results on the equivalence between the MAP and the regularized maximum likelihood, and the computation of the information criteria for model selection are available upon request.

**Table 5**
Model selection. Entries report the value of negative regularized log-likelihood ($\ell_{\text{reg}}$), i.e., the MAP, Akaike (AIC), corrected Akaike (AICc), and Bayesian (BIC) information criteria, as well the corresponding AIC, AICc, and BIC weights for 15 different calibrated HEJD models for weekly OEX observations in the period January 3, 2007–December 31, 2012. Models are calibrated using the regularized weighted non-linear least squares. The jump structure $(m, n)$, for $m, n \in \mathbb{N}$, denotes a HEJD model with $m$ distinct positive and $n$ distinct negative jump types. Models with better data fit exhibit lower values for negative log-MAP, AIC, AICc, and BIC, and higher values for the AIC, AICc, and BIC weights.

| Model $(m, n)$ | $\ell_{\text{reg}}$ | AIC | AICc | BIC | AIC Weights | AICc Weights | BIC Weights |
|---|---|---|---|---|---|---|---|
| (0,0) | 327.30 | 656.59 | 656.65 | 658.88 | 1.95e−30 | 4.60e−30 | 8.27e−28 |
| (0,1) | 261.71 | 529.42 | 529.78 | 536.28 | 0.00803 | 0.01630 | 0.34708 |
| (1,0) | 332.82 | 671.63 | 671.99 | 678.49 | 1.05e−33 | 2.14e−33 | 4.56e−32 |
| (0,2) | 265.16 | 540.33 | 541.25 | 551.75 | 0.00003 | 0.00005 | 0.00015 |
| (1,1) | 257.68 | 525.36 | 526.28 | 536.79 | 0.06116 | 0.09353 | 0.26891 |
| (2,0) | 333.80 | 677.61 | 678.53 | 689.03 | 5.32e−35 | 8.14e−35 | 2.34e−34 |
| (0,3) | 267.62 | 549.23 | 551.02 | 565.23 | 4.00e−07 | 3.98e−07 | 1.79e−07 |
| (1,2) | 253.05 | 520.11 | 521.89 | 536.10 | 0.84538 | 0.84111 | 0.37816 |
| (2,1) | 258.29 | 530.57 | 532.36 | 546.57 | 0.00451 | 0.00448 | 0.00202 |
| (3,0) | 334.62 | 683.23 | 685.02 | 699.23 | 3.19e−36 | 3.17e−36 | 1.43e−36 |
| (0,4) | 261.36 | 540.72 | 543.69 | 561.28 | 0.00003 | 0.00002 | 1.29e−06 |
| (1,3) | 253.40 | 524.80 | 527.76 | 545.37 | 0.08086 | 0.04450 | 0.00368 |
| (2,2) | 270.81 | 559.63 | 562.60 | 580.20 | 2.21e−09 | 1.22e−09 | 1.01e−10 |
| (3,1) | 268.93 | 555.85 | 558.82 | 576.42 | 1.46e−08 | 8.04e−09 | 6.65e−10 |
| (4,0) | 334.47 | 686.73 | 689.70 | 707.30 | 5.55e−37 | 3.06e−37 | 2.53e−38 |

we compare the models' in-sample performance in terms of the Akaike (AIC), the corrected Akaike (AICc) and the Bayesian (BIC) information criterion. The corresponding weights based on the relative likelihood of the models are also computed. Finally, we compute the pairwise evidence ratios.

Table 5 summarizes the average in-sample information criteria. In terms of the average negative log-maximum a posteriori loss function (neg. log-MAP), we conclude that the model (1, 2) has the best score, and it is closely followed by the models (1, 3) and (1, 1). The same results are obtained for AIC and AICc statistics. Using BIC we conclude that (1, 1) shows better performance than (1, 3), but the model (1, 2) still remains the selected one. As expected, models that completely exclude the possibility for negative jumps in the underlying asset perform very poorly.

To determine the significance of the difference between models' option pricing errors, we also consider the Diebold and Mariano (1995) test. For the in-sample (out-of-sample) exercise, the model prices are obtained by using the set of calibrated parameters on a date, which coincides with (precedes) the observation date of the quoted market option prices. The test is computed for the series of average weighted root mean square errors. For the in-sample test, given in Table 6, the hyper-exponential jump-diffusion models with jump structures (1,3) and (1,2) have the smallest mean and standard deviation estimates, respectively. The Diebold–Mariano test indicates that the HEJD(1,3) outperforms all calibrated models at all significance levels. The HEJD(1,2) significantly outperform all model, except the HEJD(1,3). However, in the case of the out-of-sample test in Table 7, results are less clear. Models with only positive jumps are clearly rejected in favor of models including negative jumps. Models with both negative and positive jumps fail to significantly outperform models with only negative jumps. The HEJD(1,3) no longer significantly outperforms the HEJD(1,2) model.

### 3.3. Exploring the HEJD(1,2) model

To obtain some intuition about the parameter values and their time variation in the sequential calibration, we explore graphically the properties of the HEJD(1, 2) model. Fig. 1, Panel A, shows the time series of conditional volatility. The average calibrated volatility $\sigma$ for the whole time span from January 3, 2007 until December 31, 2012 is 14.94 percent. We observe a sharp increase in the volatility around September 2008 reaching 65 percent. A similar behavior can be observed for the jump intensity parameter $\lambda$ in Panel B of Fig. 1. The average jump intensity is approximately 10.5 jumps per year, but varies quite a lot depending on the calibration day.

In the HEJD(1,2) model, jumps can be divided into one positive and two types of negative jumps (see Fig. 1, Panel C). The average positive jump size equals 0.22 percent, the absolute average magnitude of small negative jumps is approximately 0.40 percent, and the absolute average size of large negative jumps is 6.26 percent. Hence, negative jumps strongly dominate positive ones. Fig. 1, Panel D, represent the probabilities $p$, $q_1$, and $q_2$ of positive, small negative, and large negative jumps. These are conditional probabilities given that a jump occurs. Over the whole sample period, they average 0.40, 42.00 and 57.60 percent, respectively. Therefore, the positive jumps are not only small in magnitude, but they also have very low conditional probability of occurrence. Hence, from a practical viewpoint, they might be even negligible. In contrast, the conditional probabilities for small and large negative jumps are substantial and similar in magnitude. For large negative jump sizes, we observe a gradual increase in their conditional probability until September 2008. In the subsequent period, this probability seems to decrease again, while the probability for small negative jumps becomes large. Nevertheless, the probability for large jumps seems to be persistently high from 2010 onwards, with additional peaks around May 2010 and August 2011.

We further explore in a regression analysis how the time series of calibrated model parameters such as the volatility parameter $\sigma$, the jump intensity $\lambda$, and the average jump size $\zeta$ depend on observable market variables, such as the implied volatility, implied skewness, and implied convexity. To this end, we use as implied volatility the 1 month ATM implied volatility. For the implied skewness, we use the difference between the 10% OTM call and put implied volatilities for options with maturity of 1 month, divided by the moneyness differential ($\Delta M = 0.2$), i.e., the so-called 90/110 skewness. The implied skewness represents a measure of the asymmetry of OEX 1-month implied volatility smile. Finally, we define the implied convexity as a measure of the curvature of the implied volatility smile. We calculate the implied convexity as the second-order central difference of implied volatility curve using ATM, and 10% OTM call and put implied volatilities, divided by the squared moneyness differential.

**Table 6**
In-sample Diebold–Mariano test. We compute the in-sample weighted root mean squared errors (RMSEs) for weekly OEX observations in the period January 3, 2007–December 31, 2012. The jump structure $(m, n)$ denotes a HEJD model with $m$ distinct positive and $n$ distinct negative jump types. Panel A summarizes the mean and the standard deviation estimates of the series of weighted RMSEs. Panel B reports the pairwise Diebold–Mariano statistics for the calibrated models. Standard errors are obtained using the Newey-West estimator with optimal number of lags based on Andrews (1991) and AR(1) process. A value greater than 1.645 implies that the test model (column) outperforms the benchmark (row) at a 95% confidence interval. A value less than −1.645 implies the opposite.

Panel A: Mean and standard deviation of the in-sample weighted RMSEs

| Model | (0,0) | (0,1) | (1,0) | (0,2) | (1,1) | (2,0) | (0,3) | (1,2) | (2,1) | (3,0) | (0,4) | (1,3) | (2,2) | (3,1) | (4,0) |
|---|---|---|---|---|---|---|---|---|---|---|---|---|---|---|---|
| Mean | 3.76 | 1.51 | 3.74 | 1.49 | 1.45 | 3.75 | 1.66 | 1.38 | 1.45 | 3.74 | 1.52 | 1.35 | 1.75 | 1.56 | 3.74 |
| | (1.13) | (0.58) | (1.12) | (0.58) | (0.59) | (1.12) | (0.87) | (0.51) | (0.58) | (1.12) | (0.71) | (0.50) | (1.09) | (0.84) | (1.12) |

Panel B: Diebold–Mariano in-sample statistics of the weighted RMSEs

| Model | (0,0) | (0,1) | (1,0) | (0,2) | (1,1) | (2,0) | (0,3) | (1,2) | (2,1) | (3,0) | (0,4) | (1,3) | (2,2) | (3,1) | (4,0) |
|---|---|---|---|---|---|---|---|---|---|---|---|---|---|---|---|
| (0,0) | | 27.04 | 11.52 | 27.07 | 27.14 | 9.41 | 23.70 | 5.36 | 27.69 | 27.25 | 12.46 | 23.25 | 27.81 | 25.33 | 12.52 |
| (0,1) | | | −27.06 | 2.75 | 3.05 | −27.08 | −4.35 | 5.76 | 4.42 | −27.04 | −0.97 | 6.80 | −5.24 | −2.49 | −27.04 |
| (1,0) | | | | 27.08 | 27.14 | −5.70 | 23.68 | 27.71 | 27.26 | 3.56 | 23.22 | 27.83 | 21.77 | 25.33 | 4.62 |
| (0,2) | | | | | 2.02 | −27.10 | −4.57 | 5.12 | 3.10 | −27.07 | −1.19 | 6.15 | −5.37 | −2.72 | −27.07 |
| (1,1) | | | | | | −27.16 | −5.02 | 3.58 | 0.26 | −27.13 | −1.65 | 4.59 | −5.78 | −3.22 | −27.13 |
| (2,0) | | | | | | | 23.69 | 27.72 | 27.28 | 8.12 | 23.24 | 27.84 | 21.79 | 25.34 | 9.37 |
| (0,3) | | | | | | | | 6.08 | 5.13 | −23.66 | 2.26 | 6.48 | −2.48 | 1.63 | −23.66 |
| (1,2) | | | | | | | | | −3.84 | −27.69 | −2.75 | 3.10 | −6.52 | −4.44 | −27.70 |
| (2,1) | | | | | | | | | | −27.25 | −1.68 | 4.86 | −5.86 | −3.30 | −27.25 |
| (3,0) | | | | | | | | | | | 23.21 | 27.82 | 21.76 | 25.32 | 1.24 |
| (0,4) | | | | | | | | | | | | 3.10 | −3.68 | −1.01 | −23.21 |
| (1,3) | | | | | | | | | | | | | −6.78 | −4.87 | −27.82 |
| (2,2) | | | | | | | | | | | | | | 3.86 | −21.76 |
| (3,1) | | | | | | | | | | | | | | | −25.32 |
| (4,0) | | | | | | | | | | | | | | | |

**Table 7**
Out-of-sample Diebold–Mariano test. We compute the out-of-sample weighted root mean squared errors (RMSEs) for weekly OEX observations in the period January 3, 2007–December 31, 2012. The jump structure $(m, n)$ denotes a HEJD model with $m$ distinct positive and $n$ distinct negative jump types. Panel A summarizes the mean and the standard deviation estimates of the series of weighted RMSEs. Panel B reports the pairwise Diebold–Mariano statistics for the calibrated models. Standard errors are obtained using the Newey-West estimator with optimal number of lags based on Andrews (1991) and AR(1) process. A value greater than 1.645 implies that the test model (column) outperforms the benchmark (row) at a 95% confidence interval. A value less than −1.645 implies the opposite.

Mean and standard deviation of the out-of-sample weighted RMSEs

| Model | (0,0) | (0,1) | (1,0) | (0,2) | (1,1) | (2,0) | (0,3) | (1,2) | (2,1) | (3,0) | (0,4) | (1,3) | (2,2) | (3,1) | (4,0) |
|---|---|---|---|---|---|---|---|---|---|---|---|---|---|---|---|
| Mean | 4.39 | 2.84 | 4.41 | 2.85 | 2.84 | 4.43 | 2.97 | 2.85 | 2.84 | 4.44 | 2.90 | 2.82 | 3.05 | 2.92 | 4.45 |
| | (1.69) | (1.92) | (1.72) | (1.93) | (1.94) | (1.72) | (1.87) | (2.19) | (1.93) | (1.73) | (1.99) | (1.94) | (1.97) | (1.87) | (1.74) |

Panel B: Diebold–Mariano out-of-sample statistics of the weighted RMSEs

| Model | (0,0) | (0,1) | (1,0) | (0,2) | (1,1) | (2,0) | (0,3) | (1,2) | (2,1) | (3,0) | (0,4) | (1,3) | (2,2) | (3,1) | (4,0) |
|---|---|---|---|---|---|---|---|---|---|---|---|---|---|---|---|
| (0,0) | | 11.56 | −1.97 | 11.30 | 11.32 | −3.07 | 13.21 | 5.36 | 11.25 | −3.46 | 10.25 | 11.31 | 11.38 | 14.74 | −4.41 |
| (0,1) | | | −13.27 | −2.55 | −0.93 | −13.26 | −1.19 | −0.82 | −0.98 | −13.74 | −2.93 | 0.20 | −2.70 | −0.61 | −13.74 |
| (1,0) | | | | 12.98 | 13.02 | −4.18 | 15.05 | 5.68 | 12.93 | −7.65 | 11.69 | 12.88 | 13.12 | 16.99 | −9.31 |
| (0,2) | | | | | 0.47 | −12.96 | −0.79 | −0.69 | 1.34 | −13.24 | −1.43 | 1.54 | −2.12 | −0.09 | −13.06 |
| (1,1) | | | | | | −13.00 | −1.03 | −0.77 | −0.10 | −13.47 | −2.09 | 0.50 | −2.55 | −0.48 | −13.48 |
| (2,0) | | | | | | | 15.23 | 5.77 | 12.91 | −2.77 | 11.71 | 12.88 | 13.27 | 17.15 | −6.44 |
| (0,3) | | | | | | | | −0.39 | 1.01 | −15.56 | −0.07 | 1.20 | −2.83 | 1.10 | −15.79 |
| (1,2) | | | | | | | | | 0.78 | −5.85 | 0.38 | 0.85 | −0.17 | 0.58 | −5.92 |
| (2,1) | | | | | | | | | | −13.37 | −1.84 | 0.54 | −2.51 | −0.46 | −13.38 |
| (3,0) | | | | | | | | | | | 12.12 | 13.32 | 13.59 | 17.49 | −4.07 |
| (0,4) | | | | | | | | | | | | 2.03 | −1.38 | 0.58 | −12.16 |
| (1,3) | | | | | | | | | | | | | −2.62 | −0.65 | −13.33 |
| (2,2) | | | | | | | | | | | | | | 3.80 | −13.83 |
| (3,1) | | | | | | | | | | | | | | | −17.73 |
| (4,0) | | | | | | | | | | | | | | | |

In Table 8, we report the results from our linear regression.[21] As expected, the changes in the volatility parameter $\sigma$ are prominently driven by the changes in the implied volatility. Changes in implied skewness and convexity do have less but still a statistically significant impact. Using all three variables, we end up with an $R^2$ of more than 34 percent. The jump intensity parameter $\lambda$ is mostly driven by implied volatility and (negative) skewness. Convexity has an insignificant impact and the $R^2$ value, using all three variables, is below four percent. When we look at the conditional jump size $\zeta$, however, we find that implied convexity is the only significant variable that has a positive impact on the jump size. In contrast, unconditional jump sizes $(\lambda\zeta)$ are mainly driven by implied volatility and skewness.

As an additional exercise, we also perform a maximum likelihood estimation of the HEJD model under the physical measure using the time series of the S&P 100 returns. We calculate the log-likelihood function for each of the candidate HEJD models by summing up the logarithms of the respective probability density functions evaluated at the observed S&P 100 returns. For a given point

[21] We note that we first take differences of the relevant variables and we use robust regression based on the Huber weighting function, see Huber (1981). The reason to do so is that the errors of ordinary least-square regressions fail the Jarque–Bera test for normality.

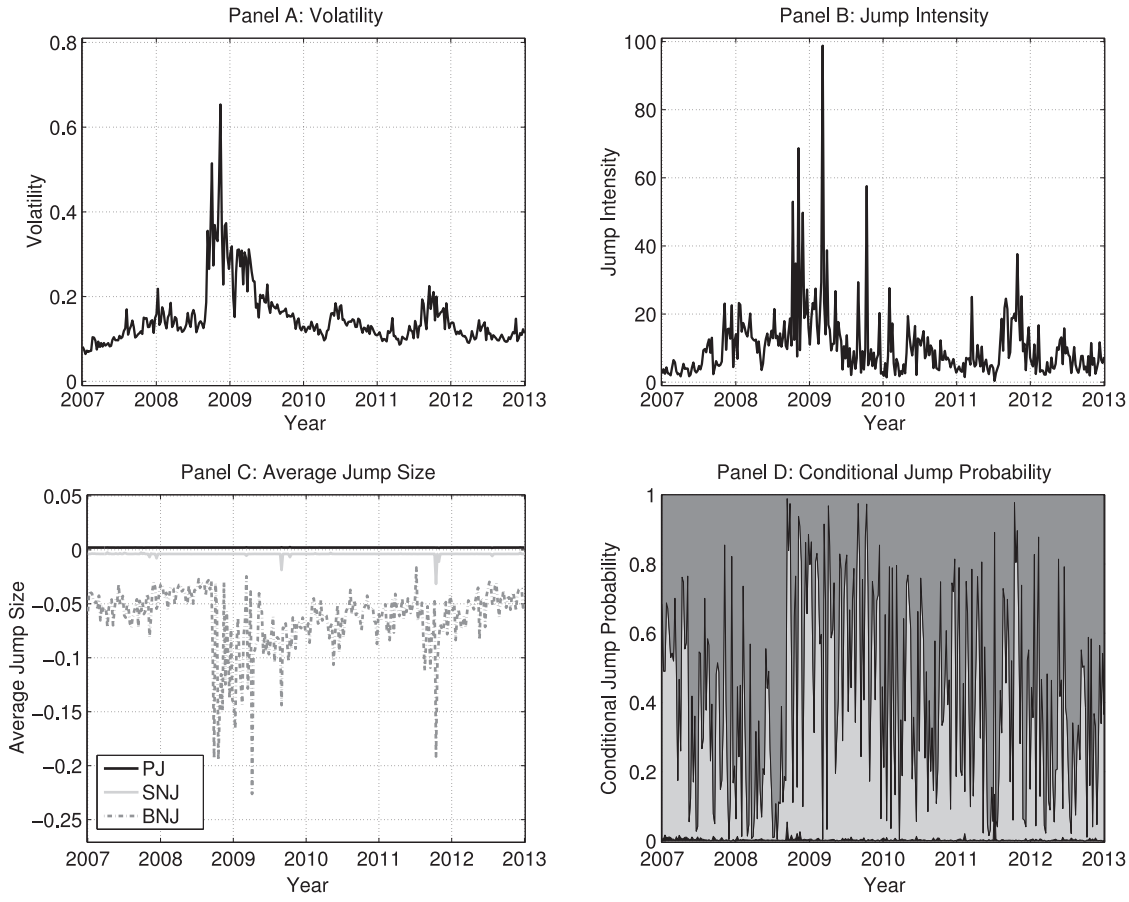


**Fig. 1.** Calibrated parameters for HEJD(1,2). Panels A and B represent the dynamics of the volatility parameter $\sigma$ and the jump intensity parameter $\lambda$. Panel C gives the dynamics of the average sizes of different jump types. Positive jumps (PJ) are represented by the solid black line, negative jump of the first kind (big negative jumps BNJ) by the dash-dot line, and the negative jump of the second kind (small negative jumps SNJ) by the solid gray line. Panel D shows an area plot for the dynamics of the conditional jump probability parameters. The black area at the bottom of the graph represents the probability for PJ, the gray area in the middle represents the probability for SNJ, and the remaining area for BNJ.

**Table 8**
Regression of changes in model parameters on changes in observable market parameters. We regress the volatility $\sigma$, the jump intensity $\lambda$, and the unconditional and conditional jump sizes $\lambda\zeta$ and $\zeta$ of the HEJD(1,2) model given in Eqs. (1)–(4) on ATM implied volatility (IV), 90/110 implied skewness (Skew), and 90/110 implied convexity (Conv), respectively, for OEX options with 1 month to maturity. We base our analysis on robust linear regression using differences and the Huber weighting function (see Huber, 1981). We report *t*-statistics in brackets.

| | Volatility ($\sigma$) | | | Jump intensity ($\lambda$) | | | Unconditional jump ($\lambda\zeta$) | | | Conditional jump ($\zeta$) | | |
|---|---|---|---|---|---|---|---|---|---|---|---|---|
| const. | 0.000 | 0.000 | 0.001 | 0.125 | 0.103 | 0.096 | −0.000 | −0.000 | −0.000 | 0.000 | 0.000 | 0.000 |
| | (0.342) | (0.352) | (0.524) | (0.389) | (0.301) | (0.273) | (−0.349) | (−0.323) | (−0.278) | (0.272) | (0.275) | (0.297) |
| IV | 0.450 | 0.481 | 0.706 | 37.898 | 26.711 | 24.740 | −0.182 | −0.160 | −0.147 | −0.084 | −0.084 | −0.037 |
| | (16.960) | (17.170) | (21.373) | (4.092) | (2.625) | (2.049) | (−15.140) | (−11.939) | (−8.557) | (−2.832) | (−2.750) | (−1.010) |
| Skew | – | 0.022 | 0.060 | – | −13.141 | −13.662 | – | 0.017 | 0.019 | – | −0.000 | 0.013 |
| | | (2.122) | (5.058) | | (−3.441) | (−3.145) | | (3.334) | (3.135) | | (−0.033) | (0.995) |
| Conv | – | – | 0.004 | – | – | −0.034 | – | – | 0.000 | – | – | 0.001 |
| | | | (9.969) | | | (-0.254) | | | (1.293) | | | (2.281) |
| Adj. $R^2$ | 0.234 | 0.245 | 0.348 | 0.007 | 0.034 | 0.033 | 0.038 | 0.059 | 0.057 | 0.004 | 0.003 | 0.021 |

in time, we compute the probability density function numerically by Fourier-inverting the respective characteristic function. Based on the log-likelihood function and the Akaike information criteria, we find that the HEJD (2,2) model provides the best fit.[22] Hence, our estimation exercise under the historical measure corroborates previous findings in the literature regarding the model selection in the HEJD framework. For instance, Sepp (2012) finds that jumps are symmetric and have two values, a small and a large jump, for both negative and positive returns. Comparing with our calibration results under the risk-neutral measure, we find that the absolute average size of negative small (large) jumps is 0.63 (2.28) percent under the historical measure. Under the risk-neutral measure, the absolute average magnitude of small negative jumps is approximately 0.40 percent, and the absolute average size of large negative jumps is 6.26 percent. Also, under the historical measure, the average size of positive small (large) jumps is 0.49 (1.98) percent. The average jump size under the risk-neutral measure for positive jumps averages only 0.22 percent. These findings reflect the concern of risk-averse investors by putting less weight on positive jumps and more weight on negative jumps.[23]

[22] However, using the BIC we find that the preferred mode is HEJD(0,2).

[23] More results on the maximum likelihood estimation of the different HEJD models can be obtained from the authors on request.

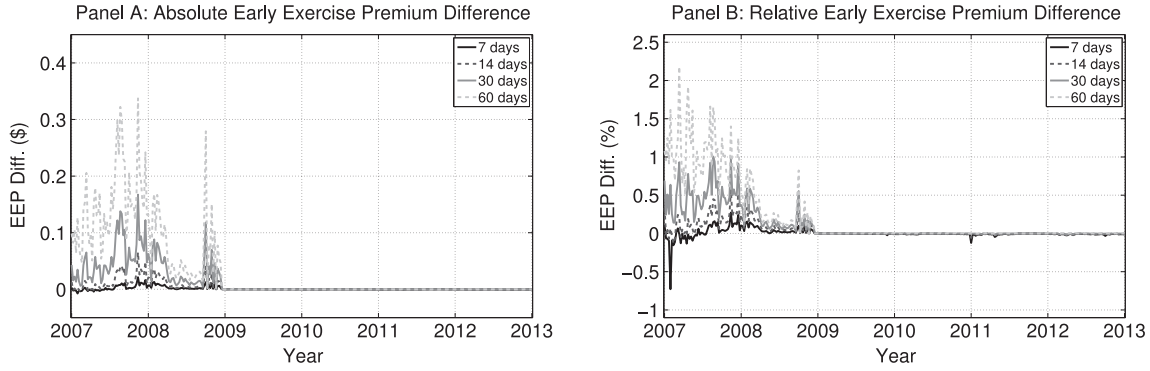


**Fig. 2.** Difference between HEJD(1,2) and BSM early exercise premiums. Panel A represents the absolute (dollar) difference between the HEJD(1,2) and the BSM-implied early exercise premium (EEP) for ATM American put options with different maturities (7, 14, 30, or 60 days). In Panel B, we plot the relative (percentage) EEP difference between the HEJD(1,2) and the BSM-implied EEP with respect to the corresponding American put option price computed using the HEJD(1,2) model. The difference (absolute and relative) is almost always positive, except for only couple of instances in the case of options with shortest maturity. The difference between the two EEPs becomes more pronounced for options with longer time to maturity.

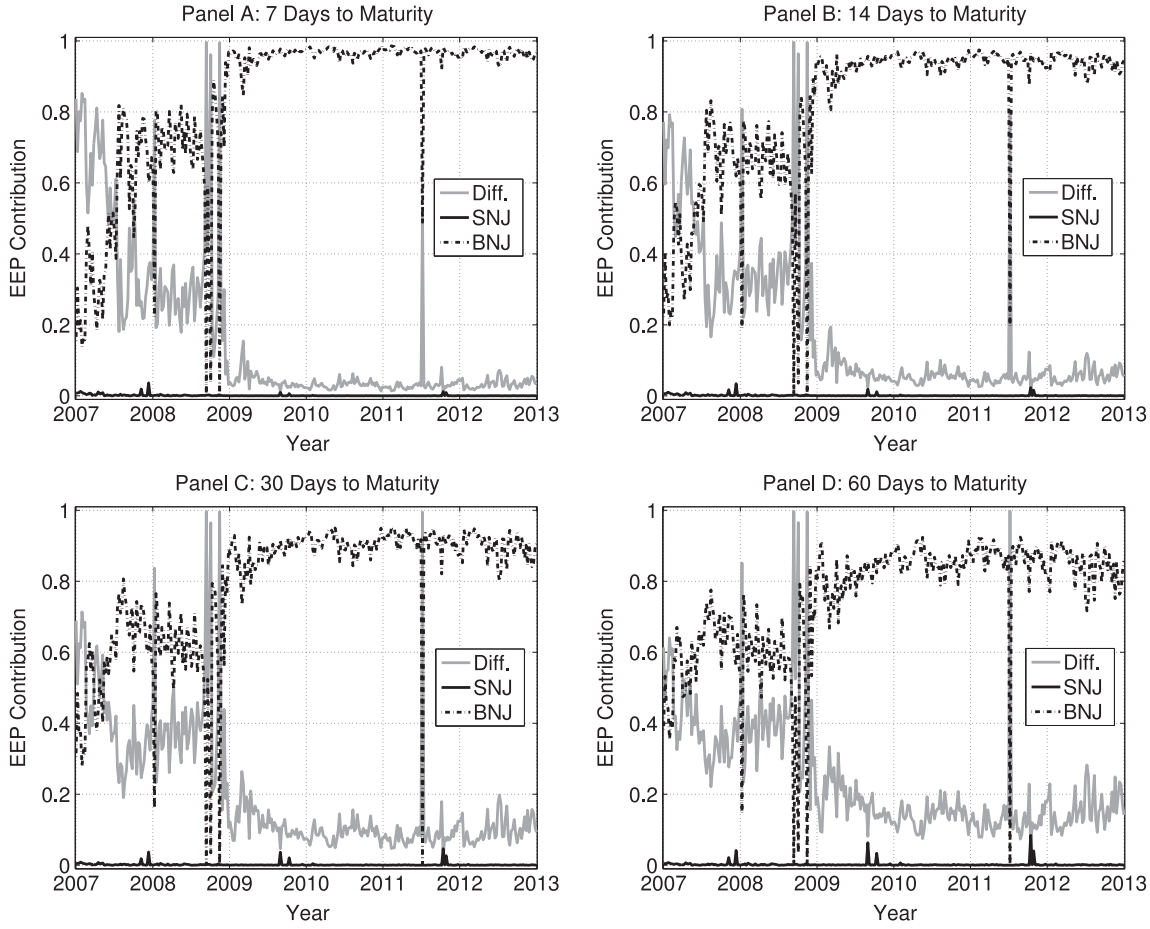


**Fig. 3.** Empirical early exercise premium disentanglement. Dynamics of the analytic disentanglement approach is presented for ATM OEX options ($M := K/F_{t,T} = 1$) given the calibrated HEJD(1,2) model parameters. In each plot solid gray line describes the portion of the early exercise premium due to the diffusion (Diff.). Solid and dash-dot black line correspond to the small (SNJ) and big (BNJ) negative jumps, respectively. Each panel corresponds to a different maturity of the ATM OEX option (7, 14, 30, or 60 days). For a given date, the contributions of diffusion, small and big jumps sum up to unity.

### *3.4. Early exercise premium and disentanglement*

To analyze the evolution of the early exercise premium (EEP) and its decomposition into diffusion and jump components we proceed in two steps. First, we compare the differences between the EEP implied by the HEJD(1,2) and the standard Black-Scholes-Merton model (BSM). While this comparison of the EEP is across two different models, we exploit in a second step our theoretical result of the jump disentanglement in Theorem 3 and analyze the EEP impact of small and large jumps within the same model, in particular within the HEJD(1,2) model.

Using the calibrated parameters from the previous section, we compute prices of both European and American options for the HEJD(1,2) model. By doing so, we obtain a time series of the HEJD(1,2)-implied EEP. Similarly, to obtain the BSM-implied EEP, we first calculate BSM implied volatilities from the market prices

of ATM American put options.[24] We then use these BSM implied volatilities to obtain the corresponding BSM ATM European put option prices, which allow us then to calculate the BSM-implied EEP.

In Fig. 2, we plot the dynamics of the absolute difference (Panel A) and the relative difference (Panel B) between the HEJD(1,2) and BSM-implied EEP for ATM options. We observe that both absolute and relative EEP differences are almost always positive, except for several observation dates at the beginning of the sample, in the case of options with shortest time to maturity. Hence, the model with jumps exhibits a higher EEP. Furthermore, the EEP difference tends to increase with maturity. However, this pattern seems to completely fade away from the end of 2008 onwards.

The above analysis uses two different models to quantify the impact of jumps. In contrast, our orthogonal decomposition of the EEP in Theorem Theorem 3 allows us to perform a similar analysis within the same model. In Fig. 3, we plot the EEP dynamics implied by the HEJD(1,2) model for different maturities. For each maturity, we plot the portion of the EEP which is due to diffusion (solid gray line), to the small jump component (solid black line), and to the large jump component (dash-dot black line). We observe similar patterns across different maturities. Small jumps have a negligible contribution except at very few isolated points in time. Again, a striking feature of the data is a structural break shortly after the start of the financial crisis in 2008. While the diffusion part played a significant role for the early exercise premium until the end of 2008, its impact decreases significantly afterwards and the premium is predominantly determined by the contribution of large jumps.

Clearly, we observe a structural change in both Fig. 2 and Fig. 3. This abrupt change is driven by extraordinarily low interest rates.[25] Starting from the end of 2008, the continuing decrease in interest rates led to a substantial reduction in the EEP. Having interest rates close to zero pushes the early exercise boundary for American put options down, which in turn significantly lowers the probability of an early exercise. The reason for absolute domination of jumps over diffusion in the post-crisis period is the following. In a relatively short period of time, which is exactly the case in our data set that consists of short-term options, the diffusion is unlikely to reach a distant early exercise boundary. On the other hand, by definition, (negative) jumps move by leaps and bounds. Hence, they have a better chance of reaching the exercise region. While the early exercise premium is close to zero in the post-crisis period, it is nevertheless possible to extract information about the importance of each process in the underlying asset price dynamics. We find that large negative jumps are by far the most important component, as they account for between 80 and 95 percent in the period from December 2008 to December 2012. The pre-crisis time window conveys different disentanglement structure and the contribution of large negative jumps varies between 20 and 80 percent. Finally, irrespectively of the time period considered, increasing time to maturity implies more importance attached to the diffusion component.

## 4. Conclusion

We price American put options in a hyper-exponential jump-diffusion framework using a maturity randomization approach. We obtain the prices of Canadized European and American options in closed form. We also obtain an analytic disentanglement of jumps and diffusion for the American early exercise premium. Given the wide spectrum of jump-diffusion models that can be accommodated within the HEJD setting, we conduct a calibration and model selection exercise using six years of data of American options on the S&P 100 index. We find that jumps play a dominant role for the early exercise of American put options by accounting on average for more than half of the early exercise premium prior to the financial crisis and more than 90 percent from December 2008 onwards.

## Appendix A. Proofs

### A1. Proof of Theorem 1: pricing of canadized european put options

The price of a European put option with strike $K$ (i.e., the log-strike is defined as $\kappa := \log(K)$) and time to maturity $\tau$ in a jump-diffusion model is the function $p := p(x, \tau)$, where $x$ is the log-price process (4), which solves the partial integro-differential equation (PIDE)

$$-\frac{\partial p}{\partial \tau}(x,\tau) + \frac{\sigma^2}{2}\frac{\partial^2 p}{\partial x^2}(x,\tau) + \mu\frac{\partial p}{\partial x}(x,\tau) - rp(x,\tau) + \lambda\int_{-\infty}^{+\infty}[p(x+y,\tau)-p(x,\tau)]f_Y(y)dy = 0, \tag{20}$$

with the boundary conditions

$$\lim_{x\downarrow-\infty} p(x,\tau) = e^{\kappa-r\tau}, \qquad \lim_{x\uparrow+\infty} p(x,\tau) = 0, \tag{21}$$

and the initial condition

$$p(x,0) = (e^{\kappa}-e^{x})^{+} := \max(e^{\kappa}-e^{x},0). \tag{22}$$

Taking the Laplace-Carson transform (LCT) in (7) of the system (20)–(22), we obtain the ordinary integro-differential equation (OIDE) for the Canadized European put option $p^* := p^*(x, \alpha)$

$$\frac{\sigma^2}{2}\frac{d^2p^*}{dx^2}(x,\alpha) + \mu\frac{dp^*}{dx}(x,\alpha) - (r+\alpha)p^*(x,\alpha) - \lambda p^*(x,\alpha) + \alpha(e^{\kappa}-e^{x})^{+} + \lambda\int_{-\infty}^{+\infty} p^*(x+y,\alpha)f_Y(y)dy = 0, \tag{23}$$

with the transformed boundary conditions

$$\lim_{x\downarrow-\infty} p^*(x,\alpha) = \frac{\alpha e^{\kappa}}{\alpha+r}, \qquad \lim_{x\uparrow+\infty} p^*(x,\alpha) = 0. \tag{24}$$

The initial condition (22) is absorbed in the Eq. (23) due to the LCT. Assuming the solution to have the form

$$p^*(x,\alpha) = \begin{cases} \sum_{l=1}^{m+1}\underline{w}_l e^{\beta_{l,r+\alpha}(x-\kappa)} + \frac{\alpha e^{\kappa}}{\alpha+r} - \frac{\alpha e^{x}}{\alpha+\delta} & \text{if } x<\kappa, \\ \sum_{l=1}^{n+1}\overline{w}_l e^{\gamma_{l,r+\alpha}(x-\kappa)} & \text{if } x\geq\kappa, \end{cases} \tag{25}$$

we obtain the coefficients $\underline{w}_1,\ldots,\underline{w}_{m+1}$ and $\overline{w}_1,\ldots,\overline{w}_{n+1}$ by analyzing the solution in the two different regions, i.e., below and above the strike price.

- The case $x < \kappa$.
  First we need to compute each of the terms in the OIDE (23). The two derivative terms are

$$\frac{dp^*}{dx}(x,\alpha) = \sum_{l=1}^{m+1}\underline{w}_l\beta_{l,r+\alpha}e^{\beta_{l,r+\alpha}(x-\kappa)} - \frac{\alpha e^{x}}{\alpha+\delta}, \quad \text{and}$$
$$\frac{d^2p^*}{dx^2}(x,\alpha) = \sum_{l=1}^{m+1}\underline{w}_l\beta_{l,r+\alpha}^2e^{\beta_{l,r+\alpha}(x-\kappa)} - \frac{\alpha e^{x}}{\alpha+\delta}. \tag{26}$$

[24] To achieve this goal, we rely on Fourier space time-stepping approach developed in Jackson et al. (2008).

[25] We recall the American put-call symmetry of Carr and Chesney (1996), which implies that an American put would not be exercised when the riskless interest rate is zero. However, their results holds only in a diffusion setting. Generalizations would require some symmetry properties for the return volatility.

The integral term is

$$\begin{aligned}
&\int_{-\infty}^{+\infty} p^*(x+y,\alpha) f_Y(y) dy \\
&= \sum_{j=1}^{n}\sum_{l=1}^{m+1} \int_{-\infty}^{0} q_j \theta_j \underline{w}_l e^{\beta_{l,r+\alpha}(x-\kappa)} e^{(\beta_{l,r+\alpha}+\theta_j)y} dy \\
&\quad + \sum_{j=1}^{n} \int_{-\infty}^{0} \left( \frac{\alpha e^{\kappa}}{\alpha+r} - \frac{\alpha e^{x+y}}{\alpha+\delta} \right) q_j \theta_j e^{\theta_j y} dy \\
&\quad + \sum_{i=1}^{m}\sum_{l=1}^{m+1} \int_{0}^{\kappa-x} p_i \eta_i \underline{w}_l e^{\beta_{l,r+\alpha}(x-\kappa)} e^{(\beta_{l,r+\alpha}-\eta_i)y} dy \\
&\quad + \sum_{i=1}^{m} \int_{0}^{\kappa-x} \left( \frac{\alpha e^{\kappa}}{\alpha+r} - \frac{\alpha e^{x+y}}{\alpha+\delta} \right) p_i \eta_i e^{-\eta_i y} dy \\
&\quad + \sum_{i=1}^{m}\sum_{l=1}^{n+1} \int_{\kappa-x}^{+\infty} p_i \eta_i \overline{w}_l e^{\gamma_{l,r+\alpha}(x-\kappa)} e^{(\gamma_{l,r+\alpha}-\eta_i)y} dy. \qquad (27)
\end{aligned}$$

After some algebra, the OIDE (23) yields the following conditions

$$\begin{aligned}
&\sum_{l=1}^{m+1} \underline{w}_l e^{\beta_{l,r+\alpha}(x-\kappa)} \left( \frac{\sigma^2}{2}\beta_{l,r+\alpha}^2 + \mu\beta_{l,r+\alpha} + \lambda\left( \sum_{i=1}^{m} \frac{p_i\eta_i}{\eta_i - \beta_{l,r+\alpha}} \right.\right. \\
&\quad \left.\left. + \sum_{j=1}^{n} \frac{q_j\theta_j}{\theta_j + \beta_{j,r+\alpha}} - 1 \right) - (\alpha+r) \right) \\
&- \sum_{l=1}^{m} \lambda p_l \eta_l e^{\eta_l(x-\kappa)} \left( \sum_{i=1}^{m+1} \frac{\underline{w}_i}{\eta_l - \beta_{i,r+\alpha}} - \sum_{j=1}^{n+1} \frac{\overline{w}_j}{\eta_l - \gamma_{j,r+\alpha}} \right. \\
&\quad \left. + \frac{1}{\eta_l} \frac{\alpha e^{\kappa}}{\alpha+r} - \frac{1}{\eta_l - 1} \frac{\alpha e^{\kappa}}{\alpha+\delta} \right) = 0. \qquad (28)
\end{aligned}$$

Using the definition of the cumulant generating function (5) and the characteristic equation, the first sum in (28) vanishes. Therefore, we obtain $m$ conditions (for $l = 1, 2, \ldots, m$) on the coefficients $\underline{w}_1, \ldots, \underline{w}_{m+1}$ and $\overline{w}_1, \ldots, \overline{w}_{n+1}$ as a system of linear equations

$$\sum_{i=1}^{m+1} \frac{\underline{w}_i}{\eta_l - \beta_{i,r+\alpha}} - \sum_{j=1}^{n+1} \frac{\overline{w}_j}{\eta_l - \gamma_{j,r+\alpha}} = \frac{1}{\eta_l - 1} \frac{\alpha e^{\kappa}}{\alpha+\delta} - \frac{1}{\eta_l} \frac{\alpha e^{\kappa}}{\alpha+r}. \qquad (29)$$

- The case $x \geq \kappa$.
  We proceed in the same way as in the previous case. The derivative terms are

$$\begin{aligned}
\frac{dp^*}{dx}(x,\alpha) &= \sum_{l=1}^{n+1} \overline{w}_l \gamma_{l,r+\alpha} e^{\gamma_{l,r+\alpha}(x-\kappa)}, \\
\frac{d^2p^*}{dx^2}(x,\alpha) &= \sum_{l=1}^{n+1} \overline{w}_l \gamma_{l,r+\alpha}^2 e^{\gamma_{l,r+\alpha}(x-\kappa)}. \qquad (30)
\end{aligned}$$

The integral term is

$$\begin{aligned}
&\int_{-\infty}^{+\infty} p^*(x+y,\alpha) f_Y(y) dy \\
&= \sum_{i=1}^{m}\sum_{l=1}^{n+1} \int_{0}^{+\infty} p_i \eta_i \overline{w}_l e^{\gamma_{l,r+\alpha}(x-\kappa)} e^{(\gamma_{l,r+\alpha}-\eta_i)y} dy \\
&\quad + \sum_{j=1}^{n}\sum_{l=1}^{n+1} \int_{\kappa-x}^{0} q_j \theta_j \overline{w}_l e^{\gamma_{l,r+\alpha}(x-\kappa)} e^{(\gamma_{l,r+\alpha}+\theta_j)y} dy \\
&\quad + \sum_{j=1}^{n}\sum_{l=1}^{m+1} \int_{-\infty}^{\kappa-x} q_j \theta_j \underline{w}_l e^{\beta_{l,r+\alpha}(x-\kappa)} e^{(\beta_{l,r+\alpha}+\theta_j)y} dy \\
&\quad + \sum_{j=1}^{n} \int_{-\infty}^{\kappa-x} \left( \frac{\alpha e^{\kappa}}{\alpha+r} - \frac{\alpha e^{x+y}}{\alpha+\delta} \right) q_j \theta_j e^{\theta_j y} dy. \qquad (31)
\end{aligned}$$

Therefore, we obtain

$$\begin{aligned}
&\sum_{l=1}^{n+1} \overline{w}_l e^{\gamma_{l,r+\alpha}(x-\kappa)} \left( \frac{\sigma^2}{2}\gamma_{l,r+\alpha}^2 + \mu\gamma_{l,r+\alpha} + \lambda\left( \sum_{i=1}^{m} \frac{p_i\eta_i}{\eta_i - \gamma_{l,r+\alpha}} \right.\right. \\
&\quad \left.\left. + \sum_{j=1}^{n} \frac{q_j\theta_j}{\theta_j + \gamma_{l,r+\alpha}} - 1 \right) - (\alpha+r) \right) \\
&+ \sum_{l=1}^{n} \lambda q_l \theta_l e^{\theta_l(x-\kappa)} \left( \sum_{i=1}^{m+1} \frac{\underline{w}_i}{\theta_l + \beta_{i,r+\alpha}} - \sum_{j=1}^{n+1} \frac{\overline{w}_j}{\theta_l + \gamma_{j,r+\alpha}} \right. \\
&\quad \left. + \frac{1}{\theta_l} \frac{\alpha e^{\kappa}}{\alpha+r} - \frac{1}{\theta_l + 1} \frac{\alpha e^{\kappa}}{\alpha+\delta} \right) = 0, \qquad (32)
\end{aligned}$$

which yields $n$ conditions (for $l = 1, \ldots, n$) on coefficients $\underline{w}_1, \ldots, \underline{w}_{m+1}$ and $\overline{w}_1, \ldots, \overline{w}_{n+1}$

$$\sum_{i=1}^{m+1} \frac{\underline{w}_i}{\theta_l + \beta_{i,r+\alpha}} - \sum_{j=1}^{n+1} \frac{\overline{w}_j}{\theta_l + \gamma_{j,r+\alpha}} = \frac{1}{\theta_l + 1} \frac{\alpha e^{\kappa}}{\alpha+\delta} - \frac{1}{\theta_l} \frac{\alpha e^{\kappa}}{\alpha+r}. \qquad (33)$$

Finally, we impose one Dirichlet condition, i.e., the value matching, and one Neumann condition, i.e., the smooth pasting, at the boundary of the two regions ($x = \kappa$):

$$\begin{aligned}
&\lim_{x\uparrow\kappa} p^*(x,\alpha) = \lim_{x\downarrow\kappa} p^*(x,\alpha), \quad \text{and} \\
&\lim_{x\uparrow\kappa} \frac{dp^*}{dx}(x,\alpha) = \lim_{x\downarrow\kappa} \frac{dp^*}{dx}(x,\alpha), \qquad (34)
\end{aligned}$$

resulting in the following two conditions:

$$\begin{aligned}
&\sum_{i=1}^{m+1} \underline{w}_i - \sum_{j=1}^{n+1} \overline{w}_j = \frac{\alpha e^{\kappa}}{\alpha+\delta} - \frac{\alpha e^{\kappa}}{\alpha+r}, \\
&\sum_{i=1}^{m+1} \beta_{i,r+\alpha} \underline{w}_i - \sum_{j=1}^{n+1} \gamma_{j,r+\alpha} \overline{w}_j = \frac{\alpha e^{\kappa}}{\alpha+\delta}. \qquad (35)
\end{aligned}$$

Finally, the conditions (29), (33), and (35) can be jointly summarized in a matrix equation

$$\mathbf{A}\mathbf{w} = \mathbf{J}, \qquad (36)$$

where

$$\mathbf{w} := \left( \underline{w}_1, \ldots, \underline{w}_{m+1}, \overline{w}_1, \ldots, \overline{w}_{n+1} \right)' \qquad (37)$$

and

$$\begin{aligned}
\mathbf{J} := \Bigg( &\kappa_\delta - \kappa_r, \kappa_\delta, \frac{\kappa_\delta}{\eta_1 - 1} - \frac{\kappa_r}{\eta_1}, \ldots, \frac{\kappa_\delta}{\eta_m - 1} - \frac{\kappa_r}{\eta_m}, \\
&\frac{\kappa_\delta}{\theta_1 + 1} - \frac{\kappa_r}{\theta_1}, \ldots, \frac{\kappa_\delta}{\theta_n + 1} - \frac{\kappa_r}{\theta_n} \Bigg)' \qquad (38)
\end{aligned}$$

are a $(n+m+2)$-dimensional column vector, and $\kappa_\rho := \frac{\alpha e^\kappa}{\alpha+\rho}$ for $\rho = \{r, \delta\}$. The matrix $\mathbf{A}$ is given by

$$\mathbf{A} := \begin{pmatrix} 1 & \cdots & 1 & -1 & \cdots & -1 \\ \beta_{1,r+\alpha} & \cdots & \beta_{m+1,r+\alpha} & -\gamma_{1,r+\alpha} & \cdots & -\gamma_{n+1,r+\alpha} \\ \frac{1}{\eta_1-\beta_{1,r+\alpha}} & \cdots & \frac{1}{\eta_1-\beta_{m+1,r+\alpha}} & -\frac{1}{\eta_1-\gamma_{1,r+\alpha}} & \cdots & -\frac{1}{\eta_1-\gamma_{n+1,r+\alpha}} \\ \vdots & \ddots & \vdots & \vdots & \ddots & \vdots \\ \frac{1}{\eta_m-\beta_{1,r+\alpha}} & \cdots & \frac{1}{\eta_m-\beta_{m+1,r+\alpha}} & -\frac{1}{\eta_m-\gamma_{1,r+\alpha}} & \cdots & -\frac{1}{\eta_m-\gamma_{n+1,r+\alpha}} \\ \frac{1}{\theta_1+\beta_{1,r+\alpha}} & \cdots & \frac{1}{\theta_1+\beta_{m+1,r+\alpha}} & -\frac{1}{\theta_1+\gamma_{1,r+\alpha}} & \cdots & -\frac{1}{\theta_1+\gamma_{n+1,r+\alpha}} \\ \vdots & \ddots & \vdots & \vdots & \ddots & \vdots \\ \frac{1}{\theta_n+\beta_{1,r+\alpha}} & \cdots & \frac{1}{\theta_n+\beta_{m+1,r+\alpha}} & -\frac{1}{\theta_n+\gamma_{1,r+\alpha}} & \cdots & -\frac{1}{\theta_n+\gamma_{n+1,r+\alpha}} \end{pmatrix}. \tag{39}$$

This concludes the proof. □

*A2. Proof of Theorem 2: pricing of canadized american put options*

The price of an American put option with strike $K$ (i.e., the log-strike is defined as $\kappa := \log(K)$) and time to maturity $\tau$ in a jump-diffusion model is the function $P := P(x, \tau)$, where $x$ is the log-return (4), which solves the free boundary problem

$$-\frac{\partial P}{\partial \tau}(x,\tau) + \frac{\sigma^2}{2}\frac{\partial^2 P}{\partial x^2}(x,\tau) + \mu\frac{\partial P}{\partial x}(x,\tau) - rP(x,\tau) + \lambda\int_{-\infty}^{+\infty}[P(x+y,\tau) - P(x,\tau)]f_Y(y)dy = 0, \tag{40}$$

with the boundary conditions

$$\begin{aligned} &\lim_{x\uparrow+\infty} P(x,\tau) = 0, \\ &\lim_{x\downarrow b_p} P(x,\tau) = e^\kappa - e^{b_p}, \\ &\lim_{x\downarrow b_p} \frac{\partial P}{\partial x}(x,\tau) = -e^{b_p}, \end{aligned} \tag{41}$$

and the initial condition

$$P(x,0) := p(x,0) = (e^\kappa - e^x)^+. \tag{42}$$

Since we work in log-returns, the early exercise boundary $B_p$ is expressed as the log-boundary $b_p := \log(B_p)$. Taking the LCT of the American option PIDE we obtain the OIDE:

$$\frac{\sigma^2}{2}\frac{d^2P^*}{dx^2}(x,\alpha) + \mu\frac{dP^*}{dx}(x,\alpha) - (r+\alpha)P^*(x,\alpha) - \lambda P^*(x,\alpha) + \alpha(e^\kappa - e^x)^+ + \lambda\int_{-\infty}^{+\infty} P^*(x+y,\alpha)f_Y(y)dy = 0, \tag{43}$$

with the new boundary conditions:

$$\begin{aligned} &\lim_{x\uparrow+\infty} P^*(x,\tau) = 0, \\ &\lim_{x\downarrow b_p^*} P^*(x,\alpha) = e^\kappa - e^{b_p^*}, \\ &\lim_{x\downarrow b_p^*} \frac{dP^*}{dx}(x,\alpha) = -e^{b_p^*}. \end{aligned} \tag{44}$$

It is important to recognize that the transformed early exercise boundary is not a non-linear function any more. Since we have applied the LCT with respect to the residual maturity $\tau$, the time dependence disappears and $b_p^*$ becomes a flat boundary. For more details on the time-independence of the early exercise boundary of a Canadized American option we refer to Carr (1998).

Given that an American option can be decomposed into its European counterpart and the early exercise premium, price of an American option in the Laplace-Carson domain can be conjectured in the form

$$P^*(x,\alpha) = \begin{cases} p^*(x,\alpha) + e_p^*(x,\alpha) & \text{if } x > b_p^*, \\ e^\kappa - e^x & \text{if } x \le b_p^*, \end{cases} \tag{45}$$

where $e_p^* := e_p(x,\alpha)$ represents the transformed early exercise premium. Furthermore, since the dynamics of the corresponding European/Canadized European and American/Canadized American options can be described by the same PIDE/OIDE, then the early exercise premium which is a difference between the two, satisfies the same equation as well. Thus, one can price American options by solving the early exercise premium OIDE

$$\frac{\sigma^2}{2}\frac{d^2e_p^*}{dx^2}(x,\alpha) + \mu\frac{de_p^*}{dx}(x,\alpha) - (r+\alpha)e_p^*(x,\alpha) + \lambda\int_{-\infty}^{+\infty}[e_p^*(x+y,\alpha) - e_p^*(x,\alpha)]f_Y(y)dy = 0, \tag{46}$$

and using the expression (45) in connection with the boundary conditions (44). Eqs. (25), (45), and (46) allow us to conjecture the EEP in the form:

$$e_p^*(x,\alpha) = \begin{cases} \sum_{l=1}^{n+1} v_l e^{\gamma_{l,r+\alpha}(x-b_p^*)} & \text{if } x > b_p^*, \\ e^\kappa - e^x - p^*(x,\alpha) & \text{if } x \le b_p^*. \end{cases} \tag{47}$$

The OIDE (43) holds in the region $x > b_p^*$. Therefore, we have the following expressions for the derivative and integral terms in the Eq. (46)

$$\begin{aligned} \frac{de_p^*}{dx}(x,\alpha) &= \sum_{l=1}^{n+1} v_l\gamma_{l,r+\alpha}e^{\gamma_{l,r+\alpha}(x-b_p^*)}, \\ \frac{d^2e_p^*}{dx^2}(x,\alpha) &= \sum_{l=1}^{n+1} v_l\gamma_{l,r+\alpha}^2 e^{\gamma_{l,r+\alpha}(x-b_p^*)}, \end{aligned} \tag{48}$$

and

$$\begin{aligned} &\int_{-\infty}^{+\infty} e_p^*(x+y,\alpha)f_Y(y)dy \\ &= \sum_{i=1}^{m}\sum_{l=1}^{n+1}\int_0^{+\infty} p_i\eta_i v_l e^{\gamma_{l,r+\alpha}(x-b_p^*)}e^{(\gamma_{l,r+\alpha}-\eta_i)y}dy \\ &\quad + \sum_{j=1}^{n}\sum_{l=1}^{n+1}\int_{b_p^*-x}^{0} q_j\theta_j v_l e^{\gamma_{l,r+\alpha}(x-b_p^*)}e^{(\gamma_{l,r+\alpha}+\theta_j)y}dy \\ &\quad - \sum_{j=1}^{n}\sum_{l=1}^{m+1}\int_{-\infty}^{b_p^*-x} q_j\theta_j \underline{w}_l e^{\beta_{l,r+\alpha}(x-\kappa)}e^{(\beta_{l,r+\alpha}+\theta_j)y}dy \\ &\quad + \sum_{j=1}^{n}\int_{-\infty}^{b_p^*-x}\left(\frac{re^\kappa}{\alpha+r} - \frac{\delta e^{x+y}}{\alpha+\delta}\right)q_j\theta_j e^{\theta_j y}dy. \end{aligned} \tag{49}$$

Solving the integrals yields

$$\begin{aligned} &\sum_{l=1}^{n+1} v_l e^{\gamma_{l,r+\alpha}(x-b_p^*)}\left(\frac{\sigma^2}{2}\gamma_{l,r+\alpha}^2 + \mu\gamma_{l,r+\alpha}\right. \\ &\quad \left. + \lambda\left(\sum_{i=1}^{m}\frac{p_i\eta_i}{\eta_i-\beta_{l,r+\alpha}} + \sum_{j=1}^{n}\frac{q_j\theta_j}{\theta_j+\beta_{j,r+\alpha}} - 1\right) - (\alpha+r)\right) \\ &\quad + \sum_{l=1}^{n}\lambda q_l\theta_l e^{\theta_l(b_p^*-x)}\left(\sum_{i=1}^{m+1}\frac{\underline{w}_i e^{\beta_{i,r+\alpha}(b_p^*-k)}}{\theta_l+\beta_{i,r+\alpha}} + \sum_{j=1}^{n+1}\frac{v_j}{\theta_l+\gamma_{j,r+\alpha}}\right. \\ &\quad \left. - \frac{1}{\theta_l}\frac{re^\kappa}{\alpha+r} + \frac{1}{\theta_l+1}\frac{\delta e^\kappa}{\alpha+\delta}\right) = 0. \end{aligned} \tag{50}$$

From this equation we obtain $n$ conditions (for $l = 1, \ldots, n$) as a system of linear equations

$$\sum_{j=1}^{n+1} \frac{v_j}{\theta_l + \gamma_{j,r+\alpha}} = \frac{1}{\theta_l}\frac{re^{\kappa}}{\alpha + r} - \frac{1}{\theta_l + 1}\frac{\delta e^{\kappa}}{\alpha + \delta} - \sum_{i=1}^{m+1} \frac{\underline{w}_i e^{\beta_{i,r+\alpha}(b_p^* - k)}}{\theta_l + \beta_{i,r+\alpha}}. \tag{51}$$

Finally, by collecting the results for European put and the early exercise premium, and applying the conditions (44), i.e., the value matching and the smooth pasting conditions at the boundary in the HEJD framework, yields

$$\begin{aligned} \sum_{j=1}^{n+1} v_j &= \frac{re^{\kappa}}{\alpha + r} - \frac{\delta e^{\kappa}}{\alpha + \delta} e^{(b_p^* - \kappa)} - \sum_{i=1}^{m+1} \underline{w}_i e^{\beta i, r+\alpha (b_p^* - \kappa)}, \\ \sum_{j=1}^{n+1} \gamma_{j,r+\alpha} v_j &= -\frac{\delta e^{\kappa}}{\alpha + \delta} e^{(b_p^* - \kappa)} - \sum_{i=1}^{m+1} \beta_{i,r+\alpha} \underline{w}_i e^{\beta i, r+\alpha (b_p^* - \kappa)}. \end{aligned} \tag{52}$$

The vector $\mathbf{v} := (v_1, \ldots, v_{n+1})'$ can be obtained by solving the matrix equation

$$\tilde{\mathbf{A}}\mathbf{v} = \tilde{\mathbf{J}}. \tag{53}$$

The $(n+1)$-dimensional column vector $\tilde{\mathbf{J}}$ is defined as

$$\tilde{\mathbf{J}} = -\boldsymbol{\Omega}\mathbf{b}_{\beta} + e^{(b_p^* - \kappa)}\boldsymbol{\omega} + \boldsymbol{\xi}, \tag{54}$$

where $\boldsymbol{\Omega}$ is $(n+1) \times (m+1)$-dimensional matrix

$$\boldsymbol{\Omega} = \begin{pmatrix} \underline{w}_1 & \underline{w}_2 & \cdots & \underline{w}_{m+1} \\ \frac{\underline{w}_1}{\theta_1 + \beta_{1,r+\alpha}} & \frac{\underline{w}_2}{\theta_1 + \beta_{2,r+\alpha}} & \cdots & \frac{\underline{w}_{m+1}}{\theta_1 + \beta_{m+1,r+\alpha}} \\ \vdots & \vdots & \ddots & \vdots \\ \frac{\underline{w}_1}{\theta_n + \beta_{1,r+\alpha}} & \frac{\underline{w}_2}{\theta_n + \beta_{2,r+\alpha}} & \cdots & \frac{\underline{w}_{m+1}}{\theta_n + \beta_{m+1,r+\alpha}} \end{pmatrix}, \tag{55}$$

and $\mathbf{b}_{\beta}$, $\boldsymbol{\omega}$, and $\boldsymbol{\xi}$ are $(n+1)$-dimensional column vectors given by

$$\begin{aligned} \mathbf{b}_{\beta} &= \left(e^{\beta_{1,r+\alpha}(b_p^* - \kappa)}, \ldots, e^{\beta_{m+1,r+\alpha}(b_p^* - \kappa)}\right)', \\ \boldsymbol{\omega} &= \left(-\frac{\delta e^{\kappa}}{\alpha + \delta}, -\frac{1}{\theta_1 + 1}\frac{\delta e^{\kappa}}{\alpha + \delta}, \ldots, -\frac{1}{\theta_n + 1}\frac{\delta e^{\kappa}}{\alpha + \delta}\right)', \quad \text{and} \\ \boldsymbol{\xi} &= \left(\frac{re^{\kappa}}{\alpha + r}, \frac{1}{\theta_1}\frac{re^{\kappa}}{\alpha + r}, \ldots, \frac{1}{\theta_n}\frac{re^{\kappa}}{\alpha + r}\right)'. \end{aligned} \tag{56}$$

The matrix $\tilde{\mathbf{A}}$ is specified as

$$\tilde{\mathbf{A}} := \begin{pmatrix} 1 & 1 & \cdots & 1 \\ \frac{1}{\theta_1 + \gamma_{1,r+\alpha}} & \frac{1}{\theta_1 + \gamma_{2,r+\alpha}} & \cdots & \frac{1}{\theta_1 + \gamma_{n+1,r+\alpha}} \\ \frac{1}{\theta_2 + \gamma_{1,r+\alpha}} & \frac{1}{\theta_2 + \gamma_{2,r+\alpha}} & \cdots & \frac{1}{\theta_2 + \gamma_{n+1,r+\alpha}} \\ \vdots & \vdots & \ddots & \vdots \\ \frac{1}{\theta_n + \gamma_{1,r+\alpha}} & \frac{1}{\theta_n + \gamma_{2,r+\alpha}} & \cdots & \frac{1}{\theta_n + \gamma_{n+1,r+\alpha}} \end{pmatrix}. \tag{57}$$

Notice that we have used only $(n+1)$ conditions so far, i.e., the value matching condition given in the first equation in (52) and the conditions (51). However, the elements of the vector $\mathbf{v}$ depend on the early exercise boundary $b_p^*$ and we have to obtain their functional form before we apply the smooth pasting condition.

The remaining smooth pasting condition given in the second equation in (52) can be rewritten in the matrix form

$$\left(\boldsymbol{\gamma}'\tilde{\mathbf{A}}^{-1}\boldsymbol{\Omega} - \boldsymbol{\beta}' \odot \underline{\mathbf{w}}'\right)\mathbf{b}_{\beta} - e^{(b_p^* - \kappa)}\left(\boldsymbol{\gamma}'\tilde{\mathbf{A}}^{-1} - \mathbf{e}_1'\right)\boldsymbol{\omega} - \boldsymbol{\gamma}'\tilde{\mathbf{A}}^{-1}\boldsymbol{\xi} = 0, \tag{58}$$

where $\underline{\mathbf{w}} := (\underline{w}_1, \ldots, \underline{w}_{m+1})'$ and $\boldsymbol{\beta} := (\beta_{1,r+\alpha}, \ldots, \beta_{m+1,r+\alpha})'$ are $(m+1)$-dimensional column vectors, and $\mathbf{e}_1 := (1, 0, \ldots, 0)'$ and $\boldsymbol{\gamma} := (\gamma_{1,r+\alpha}, \ldots, \gamma_{n+1,r+\alpha})'$ are $(n+1)$-dimensional column vectors. The symbol $\odot$ denotes the Hadamard (element-wise) product.

The critical stock price can be computed numerically via, e.g., bisection method or a similar technique. □

### A3. Proof of Theorem 3: Disentangling jumps from diffusion

The early exercise premium of a Canadized American put solves the OIDE in the continuation region, i.e., for $x > b_p^*$,

$$\begin{aligned} &\frac{\sigma^2}{2}\frac{d^2 e_p^*}{dx^2}(x,\alpha) + \mu\frac{de_p^*}{dx}(x,\alpha) - (r+\alpha)e_p^*(x,\alpha) \\ &\quad + \lambda\int_{-\infty}^{+\infty}[e_p^*(x+y,\alpha) - e_p^*(x,\alpha)]f_Y(y)dy = 0, \end{aligned} \tag{59}$$

with the boundary conditions

$$\begin{aligned} &\lim_{x\uparrow+\infty} e_p^*(x,\alpha) = 0, \\ &\lim_{x\downarrow b_p^*} e_p^*(x,\alpha) = e^{\kappa} - e^{b_p^*} - p^*(b_p^*,\alpha), \quad \text{and} \\ &\lim_{x\downarrow b_p^*}\frac{\partial e_p^*}{\partial x}(x,\alpha) = -e^{b_p^*} - \left.\frac{\partial p^*}{\partial x}\right|_{x=b_p^*}. \end{aligned} \tag{60}$$

Using the Feynman-Kac formula and the result (13) for Canadized European put options, we can express the value of the early exercise premium for an Canadized American put option as

$$\begin{aligned} &e_p^*(x,\alpha) \\ &= \mathbb{E}_x\left[e^{-(r+\alpha)(\tau_{b_p^*} - t)}\left(\frac{re^{\kappa}}{\alpha + r} - \frac{\delta e^{X_{\tau_{b_p^*}}}}{\alpha + \delta} - \sum_{i=1}^{m+1}\underline{w}_i e^{\beta_{i,r+\alpha}(X_{\tau_{b_p^*}} - \kappa)}\right)\right], \end{aligned} \tag{61}$$

where $\tau_{b_p^*}$ is the first hitting time of the flat boundary $b_p^* < \kappa$ from above for the process $X_t$ given by (4). Therefore, we have

$$\begin{aligned} e_p^*(x,\alpha) &= \frac{re^{\kappa}}{\alpha + r}\mathbb{E}_x\left[e^{-(r+\alpha)(\tau_{b_p^*} - t)}\right] \\ &\quad + \frac{\delta e^{b_p^*}}{\alpha + \delta}\mathbb{E}_x\left[e^{-(r+\alpha)(\tau_{b_p^*} - t) + (X_{\tau_{b_p^*}} - b_p^*)}\right] \\ &\quad - \sum_{i=1}^{m+1}\underline{w}_i e^{\beta_{i,r+\alpha}(b_p^* - \kappa)}\mathbb{E}_x\left[e^{-(r+\alpha)(\tau_{b_p^*} - t) + \beta_{i,r+\alpha}(X_{\tau_{b_p^*}} - b_p^*)}\right]. \end{aligned} \tag{62}$$

At this point, we introduce a notation which will help us distinguish whether the stopping of the process $X_t$ is due to the diffusion or the jumps. The events $\mathscr{E}_0 := \{X_{\tau_{b_p^*}} = b_p^*\}$ correspond to the stopping of the process $X_t$ due to the hitting of the flat boundary $b_p^*$. On the other hand, we define for all $j = 1, \ldots, n$ the events $\mathscr{E}_j := \{X_{\tau_{b_p^*}} < b_p^* \,|\, \text{the overshoot is due to the jump of type } j\}$ which represent the stopping of the process $X_t$ due to the overshoot of the flat boundary $b_p^*$.

Due to the conditional memorylessness of the hyper-exponential distribution (e.g., see Cai, 2009 and Yin et al., 2013), the following result holds in the continuation region for any $\rho \in \mathbb{R}_+$:

$$\begin{aligned} &\mathbb{E}_x\left[e^{-(\alpha+r)(\tau_{b_p^*} - t) + \rho(X_{\tau_{b_p^*}} - b_p^*)}\right] \\ &\quad = \mathbb{E}_x\left[e^{-(\alpha+r)(\tau_{b_p^*} - t)}\mathbb{1}_{\mathscr{E}_0}\right] + \sum_{j=1}^{n}\frac{\theta_j}{\theta_j + \rho}\mathbb{E}_x\left[e^{-(\alpha+r)(\tau_{b_p^*} - t)}\mathbb{1}_{\mathscr{E}_j}\right]. \end{aligned} \tag{63}$$

Using the Lemma 2.2 of Yin et al. (2013), we obtain the matrix equation

$$\mathbf{M}\boldsymbol{\epsilon} = \mathbf{b}_{\gamma}, \tag{64}$$

where $(n+1)$-dimensional column vectors $\boldsymbol{\epsilon}$ and $\mathbf{b}_\gamma$ are respectively given by

$$\boldsymbol{\epsilon} := \left(\mathbb{E}_x\left[e^{-(\alpha+r)(\tau_{b_p^*}-t)}\mathbb{1}_{\mathscr{E}_0}\right], \mathbb{E}_x\left[e^{-(\alpha+r)(\tau_{b_p^*}-t)}\mathbb{1}_{\mathscr{E}_1}\right], \ldots, \mathbb{E}_x\left[e^{-(\alpha+r)(\tau_{b_p^*}-t)}\mathbb{1}_{\mathscr{E}_n}\right]\right)', \tag{65}$$

$$\mathbf{b}_\gamma := \left(e^{\gamma_{1,r+\alpha}(x-b_p^*)}, e^{\gamma_{2,r+\alpha}(x-b_p^*)}, \ldots, e^{\gamma_{n+1,r+\alpha}(x-b_p^*)}\right)'. \tag{66}$$

Finally, $(n+1)$-dimensional square matrix $\mathbf{M}$ is defined as

$$\mathbf{M} := \begin{pmatrix} 1 & \frac{\theta_1}{\theta_1+\gamma_{1,r+\alpha}} & \frac{\theta_2}{\theta_2+\gamma_{1,r+\alpha}} & \cdots & \frac{\theta_n}{\theta_n+\gamma_{1,r+\alpha}} \\ 1 & \frac{\theta_1}{\theta_1+\gamma_{2,r+\alpha}} & \frac{\theta_2}{\theta_2+\gamma_{2,r+\alpha}} & \cdots & \frac{\theta_n}{\theta_n+\gamma_{2,r+\alpha}} \\ \vdots & \vdots & \vdots & \vdots & \vdots \\ 1 & \frac{\theta_1}{\theta_1+\gamma_{n+1,r+\alpha}} & \frac{\theta_2}{\theta_2+\gamma_{n+1,r+\alpha}} & \cdots & \frac{\theta_n}{\theta_n+\gamma_{n+1,r+\alpha}}. \end{pmatrix}. \tag{67}$$

Therefore, by calculating the vector $\boldsymbol{\epsilon}$ and by decomposition (63), we can disentangle diffusion and jump for the Canadized early exercise premium as in (62). The diffusion component is given by

$$e_{p,d}^*(x,\alpha) = \left(\frac{re^{\kappa}}{\alpha+r} - \frac{\delta e^{\kappa}}{\alpha+\delta}e^{(b_p^*-\kappa)} - \sum_{i=1}^{m+1}\underline{w}_i e^{\beta i,r+\alpha(b_p^*-\kappa)}\right) \mathbb{E}_x\left[e^{-(\alpha+r)(\tau_{b_p^*}-t)}\mathbb{1}_{\mathscr{E}_0}\right], \tag{68}$$

and the jump component can be represented as a sum of individual contribution of all jump types to the early exercise premium

$$e_{p,j}^*(x,\alpha) = \sum_{l=1}^{n} e_{p,j,l}^*(S_t,\alpha), \tag{69}$$

where[26]

$$e_{p,j,l}^*(S_t,\alpha) = \left(\frac{re^{\kappa}}{\alpha+r} - \frac{\theta_l\delta e^{\kappa}}{(\theta_l+1)(\alpha+\delta)}e^{(b_p^*-\kappa)} - \sum_{i=1}^{m+1}\frac{\theta_l}{\theta_l+\beta_{i,r+\alpha}}\underline{w}_i e^{\beta i,r+\alpha(b_p^*-\kappa)}\right) \times\mathbb{E}_x\left[e^{-(\alpha+r)(\tau_{b_p^*}-t)}\mathbb{1}_{\mathscr{E}_l}\right]. \tag{70}$$

This concludes the proof. □

## References


Abate, J., Whitt, W., 2006. A unified framework for numerically inverting laplace transforms. INFORMS J. Comput. 18, 408–421.

Aït-Sahalia, Y., 2004. Disentangling diffusion from jumps. J. Financ. Econ. 74, 487–528.

Alili, L., Kyprianou, A.E., 2005. Some remarks on first passage of Lévy processes, the American put, and pasting principles. Annals Appl Probab. 15, 2062–2080.

Andrews, D., 1991. Heteroskedasticity and autocorrelation consistent covariance matrix estimation. Econometrica 59, 817–858.

Avram, F., Chan, T., Usabel, M., 2002. On the valuation of constant barrier options under spectrally one-sided exponential Lévy models and Carr's approximation for American puts. Stoch. Process. Their Appl. 100, 75–107.

Barone-Adesi, G., Whaley, R.E., 1987. Efficient analytic approximation of American option values. J. Finance 42, 301–320.

Black, F., Scholes, M.S., 1973. The pricing of options and corporate liabilities. J. Political Econ. 81, 637–654.

Boyarchenko, S.I., Levendorskiĭ, S.Z., 2002. Non-Gaussian Merton-Black-Scholes theory. Vol. 9. Singapore: World Scientific.

Broadie, M., Detemple, J.B., 2004. Option pricing: valuation models and applications. Manage. Sci. 50, 1145–1177.

Cai, N., 2009. On first passage times of a hyper-exponential jump diffusion process. Oper. Res. Lett. 37, 127–134.

Cai, N., Sun, L., 2014. Valuation of stock loans with jump risk. J. Econ. Dyn. Control 40, 213–241.

Carr, P., 1998. Randomization and the american put. Rev. Financ. Stud. 11, 597–626.

Carr, P., Chesney, M., 1996. American put call symmetry. HEC Preprint 70, 85–112.

Chesney, M., Jeanblanc, M., 2004. Pricing american currency options in an exponential Lévy model. Appl. Math. Finance 3, 207–225.

Chiarella, C., Ziogas, A., 2009. American call options under jump-diffusion processes - a fourier transform approach. Appl. Math. Finance 16, 37–79.

Cont, R., Tankov, P., 2004. Non-parametric calibration of jump-diffusion option pricing models. J. Comput. Finance 7, 1–50.

Crosby, J., Saux, N.L., Mijatović, A., 2010. Approximating Lévy processes with a view to option prices. Int. J. Theor. Appl. Finance 13, 63–91.

Detemple, J., 2005. American-style derivatives: Valuation and Computation. CRC Press.

Diebold, F., Mariano, R.S., 1995. Comparing predictive accuracy. J. Bus. Econ. Stat. 13, 253–265.

Fang, F., Oosterlee, C.W., 2004. A novel pricing method for european options based on fourier-cosine series expansions. SIAM J. Sci. Comput. 31, 826–848.

Fang, F., Oosterlee, C.W., 2009. Pricing early-exercise and discrete barrier options by fourier-cosine series expansions. Numerische Mathematik 114, 27–62.

Gaver Jr., D.P., 1966. Observing stochastic processes, and approximate transform inversion. Oper. Res. 15, 444–459.

Hellmich, M., Kassberger, S., Schmidt, W.M., 2013. Credit modeling under jump-diffusion with exponentially distributed jumps — stable calibration, dynamics and gap risk. Int. J. Theor. Appl. Finance 16, 1–26.

Hofer, M., Mayer, P., 2013. Pricing and hedging of lookback options in hyper-exponential jump-diffusion model. Appl. Math. Finance 20, 489–511.

Huber, P.J., 1981. Robust Statistics. Hoboken, NJ: John Wiley & Sons, Inc..

Jackson, K.R., Jaimungal, S., Surkov, V., 2008. Fourier space time-stepping for option pricing with Lévy models. J. Comput. Finance 12, 1–29.

Jeannin, M., Pistorius, M., 2010. A transform approach to compute prices and greeks of barrier options driven by a class of Lévy processes. Quant. Finance 10, 629–644.

Kimura, T., 2010. Alternative randomization for valuing american options. Asia-Pacific J. Oper. Res. 27, 167–187.

Kou, S.G., 2002. A jump-diffusion model for option pricing. Manage. Sci. 48, 1086–1101.

Kou, S.G., Wang, H., 2003. First passage times of a jump diffusion process. Adv. Appl. Probab. 35, 504–531.

Kou, S.G., Wang, H., 2004. Option pricing under a double exponential jump diffusion model. Manage. Sci. 35, 1178–1192.

Kuznetsov, A., 2013. On the convergence of the gaver-stehfest algorithm. SIAM J. Numer. Anal. 51, 2984–2998.

Levendorskiĭ, S.Z., 2004a. Pricing of the american put under Lévy processes. Int. J. Theor. Appl. Finance 7, 303–335.

Levendorskiĭ, S.Z., 2004b. Early exercise boundary and option prices in Lévy driven models. Quant. Finance 4, 525–547.

Lindström, E., Ströjby, J., Brodén, M., Wiktorsson, M., Holst, J., 2008. Sequential calibration of options. Comput. Stat. Data Anal. 52, 2877–2891.

Lipton, A., 2002. Assets with jumps. Risk 15, 149–153.

Lord, et al., 2008. A fast and accurate FFT-based method for pricing early-exercise options under Lévy processes. SIAM J. Sci. Computating 30, 1678–1705.

Mordecki, E., 2002. Optimal stopping and perpetual options for Lévy processes. Finance Stochastics 6, 473–493.

Schroder, M., 1999. Changes of numeraire for pricing futures, forwards, and options. Rev. Financ. Stud. 12, 1143–1163.

Sepp, A., 2004. Analytical pricing of double-barrier options under a double-exponential jump diffusion process — applications of laplace transform. Int. J. Theor. Appl. Finance 7, 151–175.

Sepp, A., 2012. An approximate distribution of delta-hedging errors in a jump-diffusion model with discrete trading and transaction costs. Quant. Finance 12, 1119–1141.

Valkó, P.P., Abate, J., 2004. Comparison of sequence accelerators for the Gaver method of numerical Laplace transform inversion. Comput. Math. Appl. 48, 629–636.

Yin, C., Shen, Y., Wen, Y., 2013. Exit problems for jump processes with applications to dividend problems. J. Comput. Appl. Math. 245, 30–52.


[26] Note that the expectations in (68) and (70) are computed by solving matrix Eq. (64).